mini-course:

# Numerical Magnetohydrodynamics with Application to Space Physics Flows


Hans De Sterck

University of Waterloo


UNIVERSITY OF WATERLOO

uwaterloo.ca

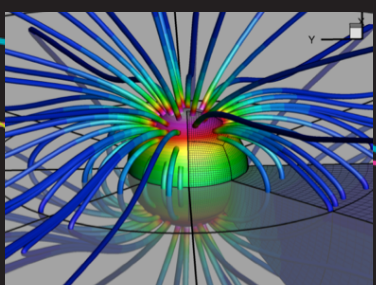

Fields Workshop on Numerical Methods for Fluid Dynamics

Carleton University, August 2013

Lecture 2: Finite Volume Methods for MHD

# this mini-course

## "Numerical Magnetohydrodynamics with Application to Space Physics Flows"

- lecture 1: Structure of MHD as a Hyperbolic System
  (conservation, waves, shocks; differences with Euler)
- lecture 2: Finite Volume Methods for MHD
  (FV methods, divergence constraint, high-order methods, adaptive cubed-sphere grids)
- lecture 3: Numerical Methods for Transonic Solutions
  (transitions from supersonic to subsonic flow (e.g., solar wind), critical points, dynamical systems methods)

(slides: goo.gl/5X5LSm )

# lecture 2: Finite Volume Methods for MHD

2.1 finite volume methods for conservation laws
(bird's eye view)

2.2 numerical strategies for $\nabla \cdot \vec{B} = 0$

2.3 high-order FV methods for MHD

2.4 adaptive cubed-sphere grids for space physics flows

# 2.1 finite volume methods for conservation laws

linear advection equation

$$\frac{\partial u}{\partial t} + a\frac{\partial u}{\partial x} = 0$$

central differences

$$\frac{u_i^{n+1} - u_i^n}{\Delta t} + a\frac{u_{i+1}^n - u_{i-1}^n}{2\Delta x} = 0$$

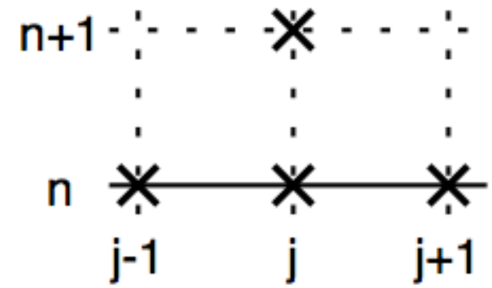


unstable!

upwind differences

$$\frac{u_i^{n+1} - u_i^n}{\Delta t} + a\frac{u_i^n - u_{i-1}^n}{\Delta x} = 0$$

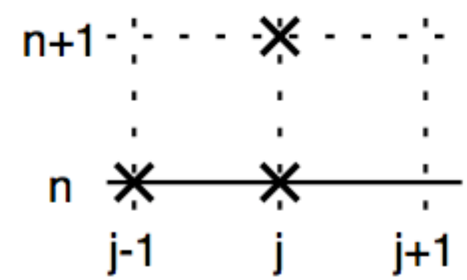


stable:

$$\Delta t < \frac{\Delta x}{a} \qquad (a > 0)$$

# conservative form

rewrite

$$\frac{u_i^{n+1} - u_i^n}{\Delta t} + a\frac{u_i^n - u_{i-1}^n}{\Delta x} = 0$$

as

$$\frac{u_i^{n+1} - u_i^n}{\Delta t} + \frac{f_{i+1/2}^{n*} - f_{i-1/2}^{n*}}{\Delta x} = 0$$

with numerical flux function

$$f_{i+1/2}^{n*} = \frac{a\,u_{i+1}^n + a\,u_i^n}{2} - \frac{1}{2}|a|(u_{i+1}^n - u_i^n)$$

conservative form: exact discrete conservation

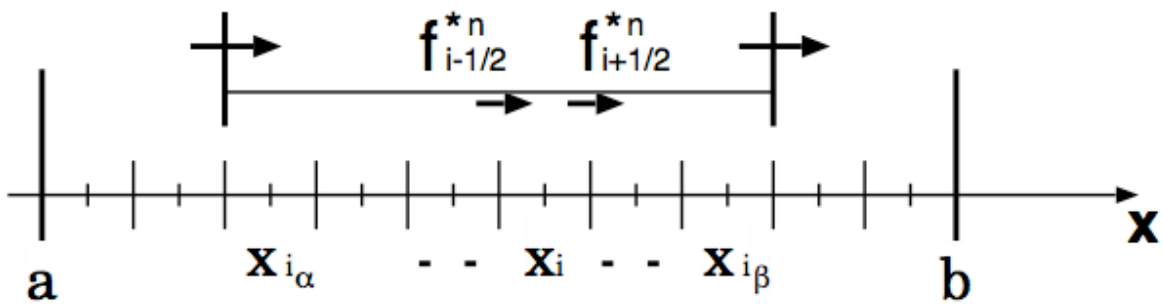


gives correct
shock speeds

# nonlinear conservation law

nonlinear flux function f(u):

$$\frac{\partial u}{\partial t} + \frac{\partial f(u)}{\partial x} = 0$$

conservative upwind method

$$\frac{u_i^{n+1} - u_i^n}{\Delta t} + \frac{f_{i+1/2}^{n*} - f_{i-1/2}^{n*}}{\Delta x} = 0$$

with numerical flux function

$$f_{i+1/2}^{n*} = \frac{f(u_{i+1}^n) + f(u_i^n)}{2} - \frac{1}{2}|f'^{n*}_{i+1/2}|(u_{i+1}^n - u_i^n)$$

# nonlinear conservative system

nonlinear system:

$$\frac{\partial \mathbf{U}}{\partial t} + \frac{\partial \mathbf{F}(\mathbf{U})}{\partial x} = 0$$

$$\frac{u_i^{n+1} - u_i^n}{\Delta t} + \frac{f_{i+1/2}^{n*} - f_{i-1/2}^{n*}}{\Delta x} = 0$$

with

$$\mathbf{F}_{i+1/2}^{n*} = \frac{\mathbf{F}(\mathbf{U}_{i+1}^n) + \mathbf{F}(\mathbf{U}_i^n)}{2} - \frac{1}{2}\max_k(|\lambda_{i+1/2}^{(k)}|)(\mathbf{U}_{i+1}^n - \mathbf{U}_i^n)$$

(flux functions: Lax-Friedrichs,
Roe (based on Jacobian eigenvalues and eigenvectors),
...)

# system in 2D: upwind finite volume method

$$\frac{\partial \mathbf{U}}{\partial t} + \nabla \cdot \vec{\mathbf{F}}(\mathbf{U}) = 0$$

$$\frac{\partial \overline{U}}{\partial t} + \oint_{\partial\Omega} \vec{F}(U) \cdot \vec{n}\, dA = 0$$

$$\overline{U} = \int_{\Omega} U\, dV$$

use integrated form over finite volume cell:

$$\frac{\partial \overline{\mathbf{U}}_{i,j}}{\partial t} + 1/\Omega_{i,j} \sum_{k=1}^{4} \vec{\mathbf{F}}^*_k \cdot \vec{n}_k\, \Delta l_k = 0$$

$$\overline{\mathbf{U}}_{i,j} = \left( \int\!\!\int \mathbf{U}(x,y,t)\, dx\, dy \right) / \Omega_{i,j}$$

(use upwind numerical fluxes F*)

2D grid with discrete unknowns:

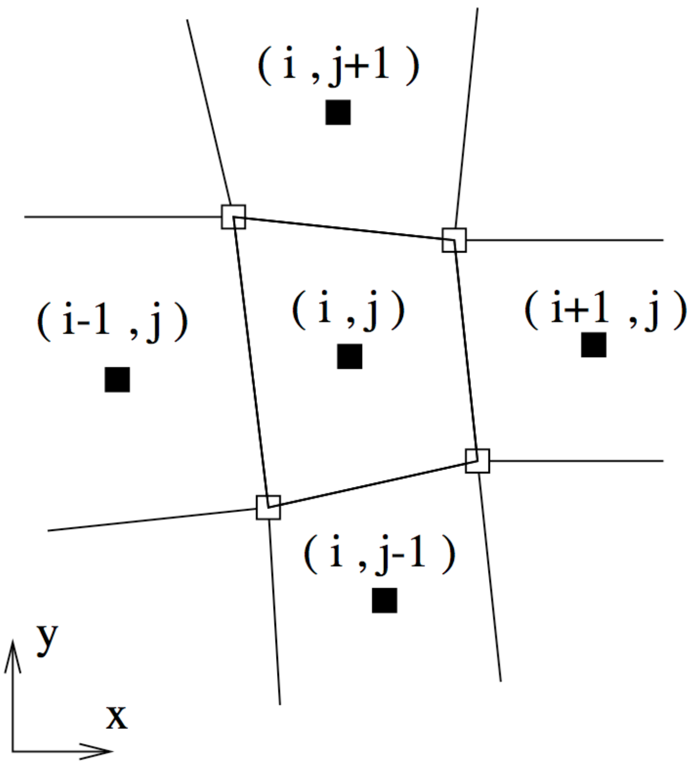


order of accuracy higher than 1:
polynomial reconstruction, limiters

# 2.2 numerical strategies for $\nabla \cdot \vec{B} = 0$

- compressible ideal MHD is a nonlinear hyperbolic conservation law, so we can use standard finite volume methods from gas dynamics!

- we need the Jacobian eigenvalues and eigenvectors

  (properly handle indeterminacies: Roe and Balsara, 1996)

- $\nabla \cdot \vec{B} = 0$ is a headache!

# the $\nabla \cdot \vec{B} = 0$ constraint in MHD

- on the analytical level:

$$\frac{\partial \vec{B}}{\partial t} = \nabla \times (\vec{v} \times \vec{B}) \quad \rightarrow \quad \frac{\partial \nabla \cdot \vec{B}}{\partial t} = 0$$

$\nabla \cdot \vec{B} = 0$ as an initial condition should suffice!

- in numerical methods:

due to discretization/rounding errors:
this may (and typically does) lead to
severe numerical instabilities!

$$\frac{\partial \nabla \cdot \vec{B}}{\partial t} = \epsilon$$

- consider remedies (similar to incompressible flow, Maxwell, ...)

# 2.2.1 projection

- solve a scalar elliptic PDE in every time step to make the magnetic field divergence-free

$$\vec{B}_{new} = \vec{B} + \nabla\phi$$

$$\nabla \cdot \vec{B}_{new} = 0 = \nabla \cdot \vec{B} + \nabla \cdot \nabla\phi$$

$$\Delta\phi = -\nabla \cdot \vec{B}$$

- works, but elliptic correction is not natural in hyperbolic system solver (upstream perturbations, elliptic operator couples solution variable in entire domain, expensive, ...)

# 2.2.2 Powell's 8-wave solver (source term)

$$\frac{\partial}{\partial t}\begin{bmatrix}\rho \\ \rho\vec{v} \\ \frac{\rho v^2}{2}+\frac{p}{\gamma-1}+\frac{B^2}{2} \\ \vec{B}\end{bmatrix}+\nabla\cdot\begin{bmatrix}\rho\vec{v} \\ \rho\vec{v}\vec{v}+\left(p+\frac{B^2}{2}\right)\vec{I}-\vec{B}\vec{B} \\ \left(\frac{\rho v^2}{2}+\frac{p}{\gamma-1}+p\right)\vec{v}-(\vec{v}\times\vec{B})\times\vec{B} \\ \vec{v}\vec{B}-\vec{B}\vec{v}\end{bmatrix}=0$$

$$\mathrm{A}_V=\begin{bmatrix} v_x & \rho & 0 & 0 & 0 & 0 & 0 & 0 \\ 0 & v_x & 0 & 0 & 0 & B_y/\rho & B_z/\rho & 1/\rho \\ 0 & 0 & v_x & 0 & 0 & -B_x/\rho & 0 & 0 \\ 0 & 0 & 0 & v_x & 0 & 0 & -B_x/\rho & 0 \\ 0 & 0 & 0 & 0 & 0 & 0 & 0 & 0 \\ 0 & B_y & -B_x & 0 & 0 & v_x & 0 & 0 \\ 0 & B_z & 0 & -B_x & 0 & 0 & v_x & 0 \\ 0 & c^2\rho & 0 & 0 & 0 & 0 & 0 & v_x \end{bmatrix}$$

$\lambda_1 = v_x + c_{fx}$ : fast wave, right

$\lambda_2 = v_x - c_{fx}$ : fast wave, left

$\lambda_3 = v_x + c_{Ax}$ : Alfvén wave, right

$\lambda_4 = v_x - c_{Ax}$ : Alfvén wave, left

$\lambda_5 = v_x + c_{sx}$ : slow wave, right

$\lambda_6 = v_x - c_{sx}$ : slow wave, left

$\lambda_7 = v_x$ : entropy wave

$\lambda_8 = 0$ : not Galilean invariant!!

UNIVERSITY OF WATERLOO

# add ‘Powell source term’

$$\boxed{\frac{\partial U}{\partial t} + \frac{\partial F(U)}{\partial x} = S}$$

$$S = -\begin{bmatrix} 0 \\ B_x \\ B_y \\ B_z \\ v_x \\ v_y \\ v_z \\ \vec{v} \cdot \vec{B} \end{bmatrix} \nabla \cdot \vec{B}$$

$$A'_V = \begin{bmatrix} v_x & \rho & 0 & 0 & 0 & 0 & 0 & 0 \\ 0 & v_x & 0 & 0 & 0 & B_y/\rho & B_z/\rho & 1/\rho \\ 0 & 0 & v_x & 0 & 0 & -B_x/\rho & 0 & 0 \\ 0 & 0 & 0 & v_x & 0 & 0 & -B_x/\rho & 0 \\ 0 & 0 & 0 & 0 & v_x & 0 & 0 & 0 \\ 0 & B_y & -B_x & 0 & 0 & v_x & 0 & 0 \\ 0 & B_z & 0 & -B_x & 0 & 0 & v_x & 0 \\ 0 & c^2\rho & 0 & 0 & 0 & 0 & 0 & v_x \end{bmatrix}$$

$\lambda_i,\ i = 1..7$ remain unchanged

$\lambda_8 = v_x$ : Galilean invariant!!

- eighth wave advects divergence error
- can be derived from ‘physical form’ of MHD equations without assuming $\nabla \cdot \vec{B} = 0$
- non-conservative source term: Toth showed RH may be violated

# 2.2.3 'constrained transport'

$\Rightarrow$ divergence-free: $\nabla \cdot \vec{B} = 0$ (or $\oint \vec{B} \cdot \vec{n} dS = 0$)

- $\vec{B}$ magnetic field (plasma ...)
- no magnetic monopoles
- also numerically, avoid magnetic monopoles at the discrete level:

  Constrained Transport (CT) approach

$\Rightarrow$ CT was known on structured grids (Evans & Hawley 1988, earlier for EM)

$\Rightarrow$ De Sterck, AIAA CFD paper 2001-2623: how to do constrained transport on unstructured grids

# CT: general idea

Faraday: $\dfrac{\partial \vec{B}}{\partial t} = \nabla \times (\vec{v} \times \vec{B})$

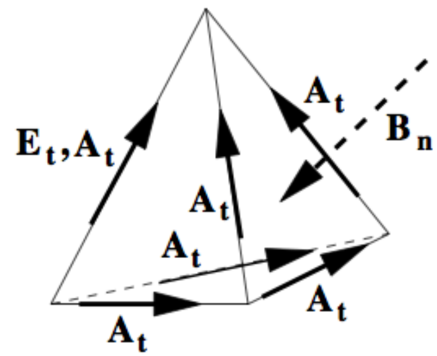


(2) $$\frac{\partial \int \vec{B} \cdot \vec{n} dS}{\partial t} = \oint (\vec{v} \times \vec{B}) \cdot d\vec{l}$$

$$\int \vec{B} \cdot \vec{n} dS = \bar{B}_n \Delta S \quad \Rightarrow \quad \frac{\partial \bar{B}_n}{\partial t} = \oint (\vec{v} \times \vec{B}) \cdot d\vec{l} \,/\, \Delta S$$

= time evolution of flux through surface

= time evolution of average normal component $\bar{B}_n$ of $\vec{B}$

$\Rightarrow \oint \vec{B} \cdot \vec{n} dS = 0$ on discrete level!!

because boundary of boundary vanishes (or contributions cancel)

# CT on structured grids

$$\frac{\partial \int_1^2 \vec{B} \cdot \vec{n} dl}{\partial t} = \frac{\partial \bar{B}_n}{\partial t} \Delta l = (\vec{v} \times \vec{B})_2 - (\vec{v} \times \vec{B})_1$$

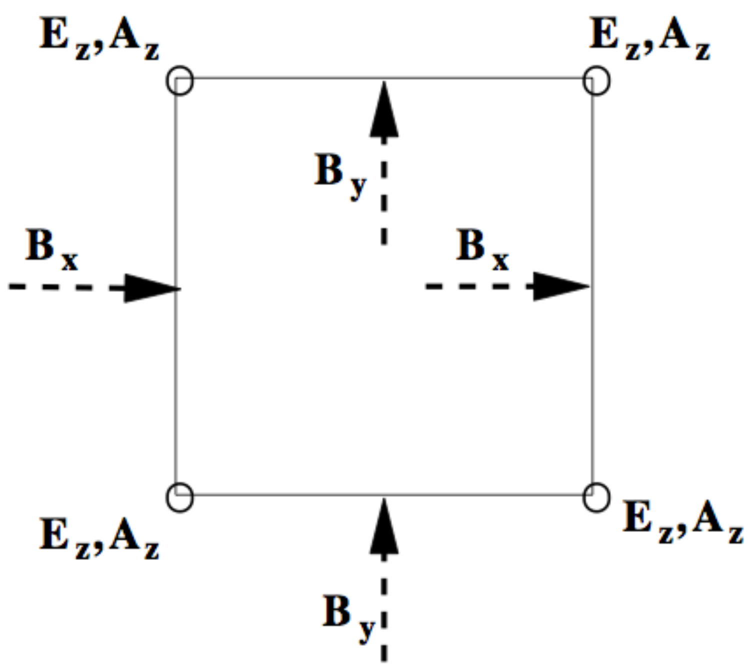


$B_x$ and $B_y$ reconstruct $\vec{B}$ in nodes

= CT (Evans & Hawley 1988)

# CT on unstructured grids

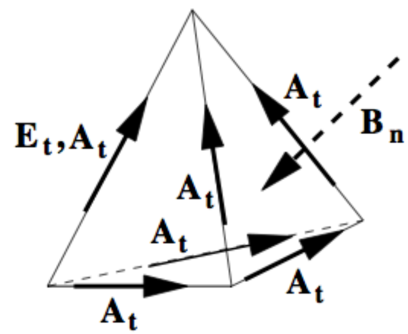


- represent $\vec{B}$ by $\bar{B}_n$: normal component on surfaces
- on unstructured grids, $\vec{B}$ can be reconstructed everywhere in the domain using vector basis functions (face elements for $\vec{B}$)
- update $\bar{B}_n$ using MU schemes (via MU interpolation of the reconstructed fields)
- this conserves the $\nabla \cdot \vec{B} = 0$ constraint at the discrete level up to machine accuracy
- this is tested for Faraday, Shallow Water MHD (system MUCT scheme)
- easy extensions: 2nd order (blended scheme), MHD, 3D, ...

= generalization of CT to multi-dimensional methods on unstructured grids

UNIVERSITY OF WATERLOO

# need vector basis functions

($\sim$ face elements, from EM, e.g. Jin 93; Robinson & Bochev 2001 for MHD)

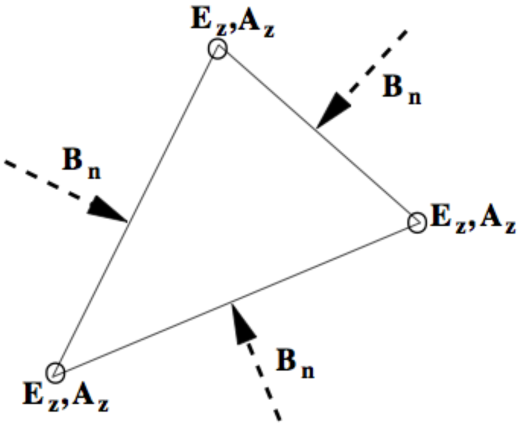


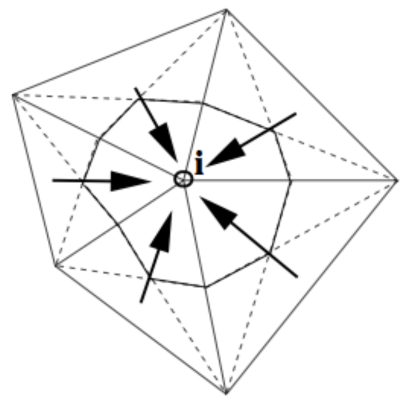


(1) reconstruct $\vec{B}$ in cell from $\bar{B}_n$ as

$$\vec{B}_{cell} = \sum_{j=1}^{3} \vec{P}_j \, B_{n,j}$$

(2) average $\vec{B}_{cell}$ to nodal $\vec{B}_i$ in upwind way

e.g. $\vec{P}_1$: normal component $\vec{P}_{1,n}$ constant on edge 1, vanishing on other edges

# magnetic field representation

$$\vec{B}_{cell} = \sum_{j=1}^{3} \vec{P}_j \, B_{n,j}$$

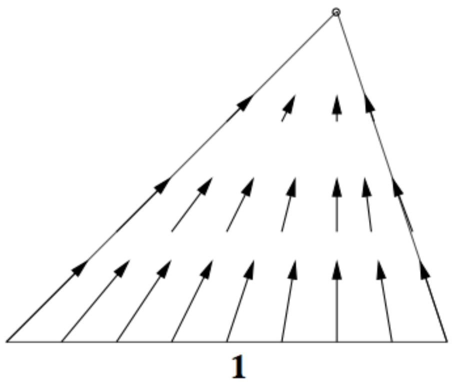


$\vec{P}_1$

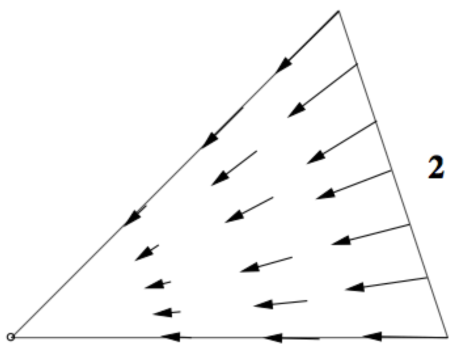


$\vec{P}_2$

e.g. $\vec{P}_1$: normal component $\vec{P}_{1,n}$ constant on edge 1, vanishing on other edges

(also higher order, quads, . . .: general concept)

# magnetic field representation

$$\vec{B}_{cell} = \sum_{j=1}^{3} \vec{P}_j \, B_{n,j}$$

- $B_{n,j}$ such that $\nabla \cdot \vec{B} =$ constant $\equiv 0$ everywhere inside element
- $B_n$ is continuous at element interfaces, so there also $\nabla \cdot \vec{B} = 0$

$\Rightarrow$ finite-element reconstructed solution satisfies $\nabla \cdot \vec{B} = 0$ everywhere!

in triangle, for lowest order element:

$\vec{B}$ constant in space, $B_n$ continuous

(on quad, or for higher order vector basis function:

$\vec{B}$ not constant in space, $B_n$ continuous)

# interpretation: differential geometry

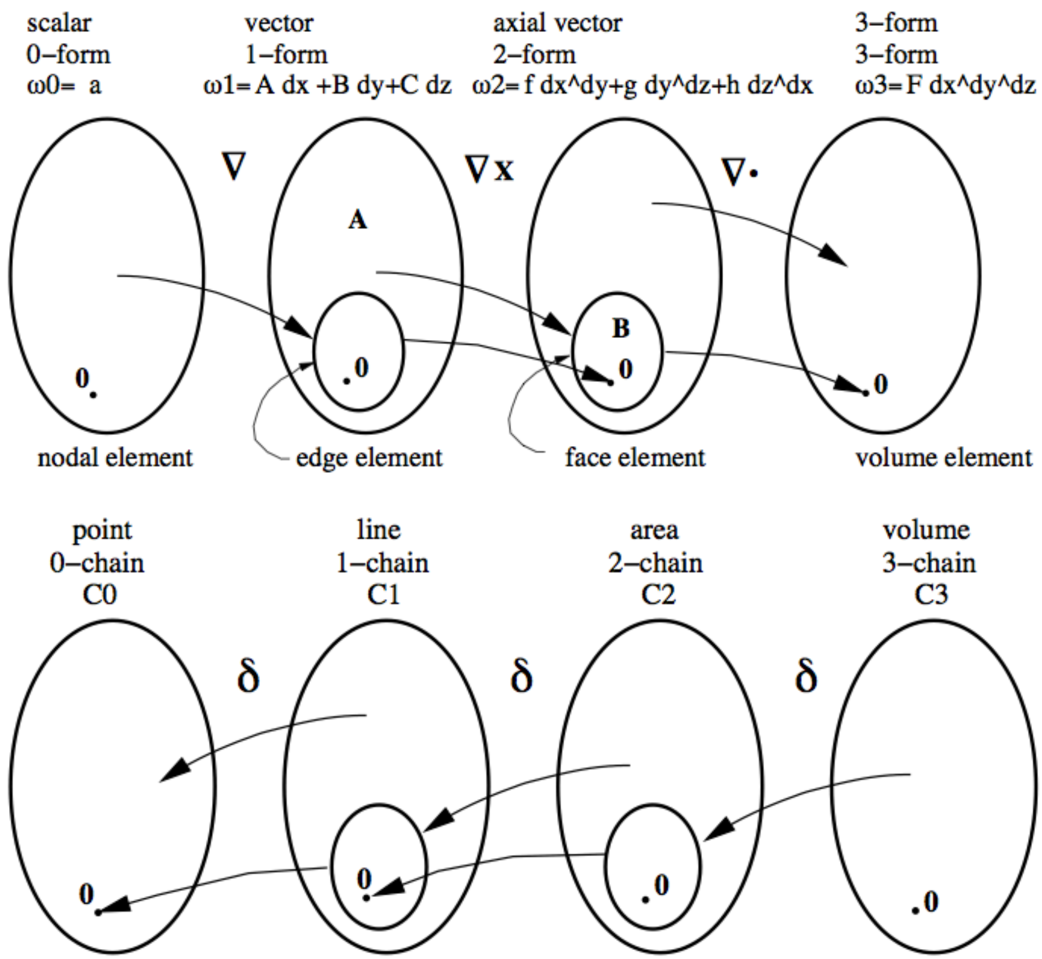


- physics = geometry
- numerics = geometry

$\Rightarrow$ in a consistent way!

also:
-mimetic schemes
-Raviart-Thomas elements
-compatible discretizations
-...

# application to ‘shallow water MHD’

(Gilman, ApJ 2000; De Sterck, Phys. Plasmas 2001)

$$\frac{\partial h}{\partial t} + \nabla \cdot (h\,\vec{v}) = 0$$

$$\frac{\partial \vec{v}}{\partial t} + (\vec{v} \cdot \nabla)\vec{v} - (\vec{B} \cdot \nabla)\vec{B} + g\,\nabla h = 0$$

$$\frac{\partial \vec{B}}{\partial t} + (\vec{v} \cdot \nabla)\vec{B} - (\vec{B} \cdot \nabla)\vec{v} = 0$$

$$\nabla \cdot (h\,\vec{B}) = 0$$

- from MHD: incompressible, 2D variation, magnetohydrostatic equilibrium
- 4 wave modes: 2 magneto-gravity waves (nonlinear), 2 Alfvén waves (linear)
- one spurious ‘div(B)’-wave (MHD!)

# SMHD Riemann problem

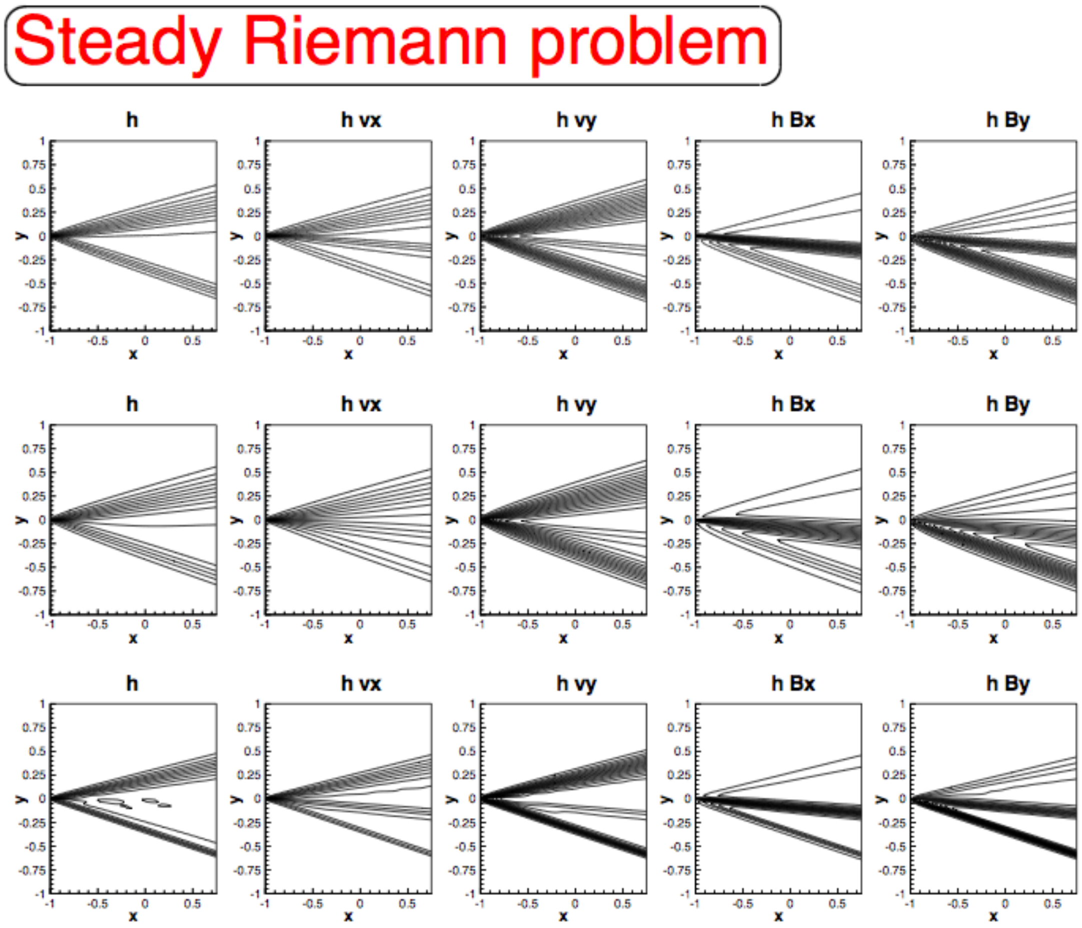

# divergence of magnetic field

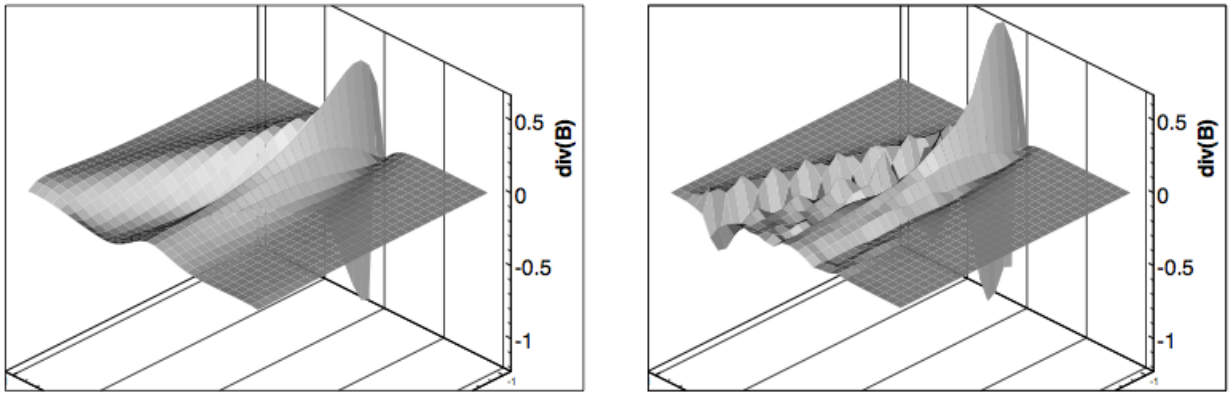


$\nabla \cdot \vec{B}$ for the first order (left) and second order (right) Lax-Friedrichs simulation of the steady Riemann problem on a grid of $30 \times 30$ finite volumes.

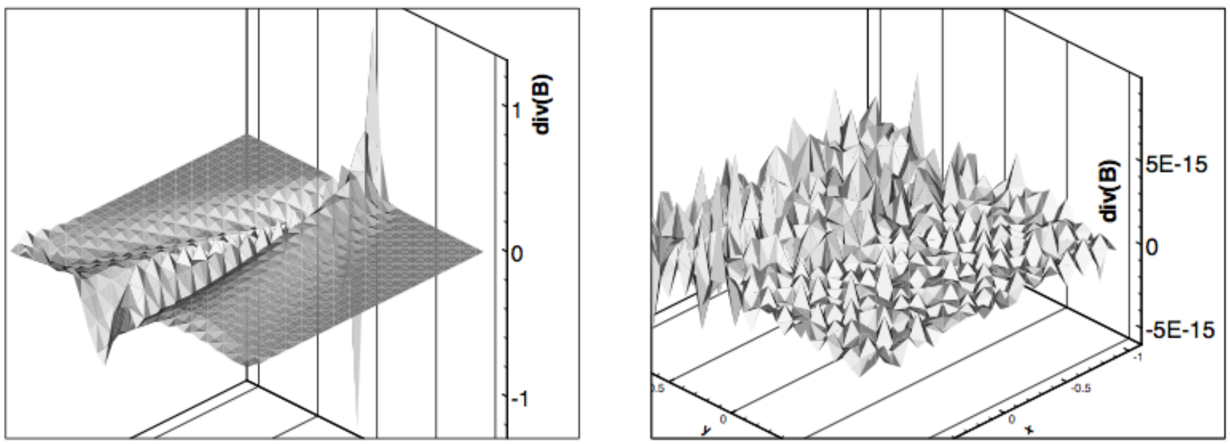


$\nabla \cdot \vec{B}$ for the full system N (left) and system N MUCT (right) simulation of the steady Riemann problem on a grid of $31 \times 31$ nodes.

➔ this works well, but may be cumbersome to implement

# 2.2.4 'generalized Lagrange multipliers' (GLM)

- Dedner et al., JCP, 2002

  (earlier work on this technique for Maxwell by Munz et al.)

- general approach

$$\frac{\partial \vec{B}}{\partial t} + \nabla \cdot (\vec{v}\vec{B} - \vec{B}\vec{v}) + \nabla\psi = 0,$$

$$\frac{\partial \psi}{\partial t} + c_h^2 \nabla \cdot \vec{B} = -\frac{c_h^2}{c_p^2}\psi.$$

('mixed hyperbolic-parabolic' variant; provides advection and diffusion for $\nabla \cdot \vec{B}$ )

$$\partial_{tt}^2 \psi + \frac{c_h^2}{c_p^2}\partial_t \psi - c_h^2 \Delta \psi = 0$$

(telegraph equation; same for $\nabla \cdot \vec{B}$ )

# GLM for MHD

$$\frac{\partial \vec{B}}{\partial t} + \nabla \cdot (\vec{v}\vec{B} - \vec{B}\vec{v}) + \nabla \psi = 0,$$

$$\frac{\partial \psi}{\partial t} + c_h^2 \nabla \cdot \vec{B} = -\frac{c_h^2}{c_p^2} \psi.$$

- eigenvalues:

$$\lambda_1 = -c_h, \quad \lambda_2 = u_x - c_f, \quad \lambda_3 = u_x - c_a, \quad \lambda_4 = u_x - c_s, \quad \lambda_5 = u_x,$$
$$\lambda_6 = u_x + c_s, \quad \lambda_7 = u_x + c_a, \quad \lambda_8 = u_x + c_f, \quad \lambda_9 = c_h.$$

- parameter choice: $c_h = \max_{i,j}(|v_n| + c_{f_n})$

$$c_r = c_p^2 / c_h = 0.18$$

# integrating the source term contribution

$$\frac{\partial \psi}{\partial t} + c_h^2 \nabla \cdot \vec{B} = -\frac{c_h^2}{c_p^2}\psi$$

1. source term integration:

$$\frac{d}{dt}\left(\iint_{\mathcal{A}_{i,j}} \psi \, dA\right) = -c_h^2 \left(\iint_{\mathcal{A}_{i,j}} \nabla \cdot \vec{B} \, dA\right) - \frac{c_h^2}{c_p^2}\left(\iint_{\mathcal{A}_{i,j}} \psi \, dA\right)$$

$$\frac{d\overline{\psi}_{i,j}}{dt} = -\frac{1}{A_{i,j}} \sum_{l=1}^{4} \sum_{m=1}^{N_g} (\omega \vec{\mathbf{f}}_{num} \cdot \vec{n} \Delta l)_{i,j,l,m} - \frac{c_h^2}{c_p^2} \overline{\psi}_{i,j}$$

2. operator splitting: first solve without source term, then update using $\frac{d\overline{\psi}_{i,j}}{dt} = -\frac{c_h^2}{c_p^2} \overline{\psi}_{i,j}$

   – advantage: no additional time step restriction from source term

   – potential disadvantage: operator splitting may decrease order of accuracy (?)

# operator splitting error for GLM

Journal of Computational Physics 250 (2013) 141–164

High-order central ENO finite-volume scheme for ideal MHD

A. Susanto[a], L. Ivan[a,*], H. De Sterck[a], C.P.T. Groth[b]

$$\frac{\partial \mathbf{U}}{\partial t} + \mathbb{A}_c \frac{\partial \mathbf{U}}{\partial x} + \mathbb{B}_c \frac{\partial \mathbf{U}}{\partial y} + \mathbb{C}_c \mathbf{U} = 0$$

let $\mathbb{D}_c = \mathbb{A}_c \frac{\partial}{\partial x} + \mathbb{B}_c \frac{\partial}{\partial y}$

using Taylor expansion, one can show that the splitting error is given by

$$\mathbf{E} = \frac{1}{2}\Delta t^2 (\mathbb{D}_c\mathbb{C}_c - \mathbb{C}_c\mathbb{D}_c)\mathbf{U} + O(\Delta t^3)$$

(see, e.g., Leveque, 2002)

where $\mathbf{U}$ is the <u>exact</u> solution.

we find

$$(\mathbb{D}_c\mathbb{C}_c - \mathbb{C}_c\mathbb{D}_c)\mathbf{U} = \frac{c_h^2}{c_p^2}\begin{bmatrix} 0 \\ 0 \\ 0 \\ \frac{\partial \psi}{\partial x} \\ \frac{\partial \psi}{\partial y} \\ 0 \\ 0 \end{bmatrix} - \frac{c_h^4}{c_p^2}\begin{bmatrix} 0 \\ 0 \\ 0 \\ 0 \\ 0 \\ 0 \\ \frac{\partial B_x}{\partial x} + \frac{\partial B_y}{\partial y} \end{bmatrix} = 0$$

# operator splitting error for GLM

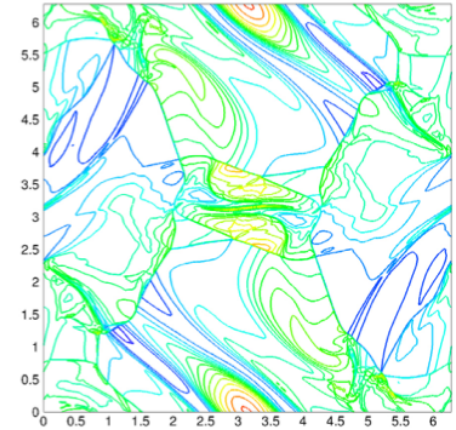


Journal of Computational Physics 250 (2013) 141–164

**High-order central ENO finite-volume scheme for ideal MHD**

A. Susanto [a], L. Ivan [a,*], H. De Sterck [a], C.P.T. Groth [b]

$$\mathbf{E} = \frac{1}{2}\Delta t^2(\mathbb{D}_c\mathbb{C}_c - \mathbb{C}_c\mathbb{D}_c)\mathbf{U} + O(\Delta t^3)$$

where $\mathbf{U}$ is the exact solution.
we find

$$(\mathbb{D}_c\mathbb{C}_c - \mathbb{C}_c\mathbb{D}_c)\mathbf{U} = \frac{c_h^2}{c_p^2}\begin{bmatrix} 0 \\ 0 \\ 0 \\ \frac{\partial\psi}{\partial x} \\ \frac{\partial\psi}{\partial y} \\ 0 \\ 0 \end{bmatrix} - \frac{c_h^4}{c_p^2}\begin{bmatrix} 0 \\ 0 \\ 0 \\ 0 \\ 0 \\ 0 \\ \frac{\partial B_x}{\partial x} + \frac{\partial B_y}{\partial y} \end{bmatrix} = 0$$

since $\psi(x,y,t) = 0$ and $\nabla \cdot \vec{B}(x,y,t) = 0$
(and then entire splitting error vanishes)

consequences:
- operator splitting does not degrade accuracy
- no need to discretize $\psi$ with high-order accuracy

# GLM

$$\frac{\partial \vec{B}}{\partial t} + \nabla \cdot (\vec{v}\vec{B} - \vec{B}\vec{v}) + \nabla \psi = 0,$$

$$\frac{\partial \psi}{\partial t} + c_h^2 \nabla \cdot \vec{B} = -\frac{c_h^2}{c_p^2}\psi.$$

- fits nicely into hyperbolic code
- *automatically handles grid resolution changes*
- *can naturally be done with high order accuracy*
- *just one extra equation, but* $\psi$ *can be discretized with low accuracy*
- *operator splitting for source term does not degrade accuracy*

Journal of Computational Physics 250 (2013) 141–164

High-order central ENO finite-volume scheme for ideal MHD

A. Susanto [a], L. Ivan [a,*], H. De Sterck [a], C.P.T. Groth [b]

# 2.3 high-order FV methods for MHD

Journal of Computational Physics 250 (2013) 141–164

High-order central ENO finite-volume scheme for ideal MHD

A. Susanto [a], L. Ivan [a,*], H. De Sterck [a], C.P.T. Groth [b]

## Overview Idea of the High-Order MHD Algorithm

- Apply a high-order **CENO** approach (Ivan & Groth, 2007, 2011) (initially proposed for 2D inviscid and viscous flows, but not for MHD) to estimate accurately the residual
- Use **CENO + GLM-MHD** (Dedner *et al.*, 2002) to satisfy $\nabla \cdot \vec{B} = 0$
- GLM source term can be integrated analytically, but not Powell's term!

  $\Rightarrow$ GLM better suited for high-order accuracy

(CENO = central essentially non-oscillatory)

# High-Order Finite-Volume Formulation

## General System of Hyperbolic Conservation Laws

$$\frac{\partial \mathbf{U}}{\partial t} + \vec{\nabla} \cdot \vec{\mathbf{F}} = \mathbf{S} + \mathbf{Q}$$

## Semi-Discrete Integral Form for a Hexahedral Element

$$\frac{d\overline{\mathbf{U}}_{i,j,k}}{dt} = -\frac{1}{V_{i,j,k}} \oint_{\partial \mathcal{V}} \vec{\mathbf{F}} \cdot \vec{n}\, da + \frac{1}{V_{i,j,k}} \iiint_{\mathcal{V}} (\mathbf{S} + \mathbf{Q})\, dv = \mathbf{R}_{i,j,k}(\overline{\mathbf{U}})$$

## Primary Steps to Obtaining Numerical Solution

- **Solution reconstruction**:
  - Approximate solution with high-order piecewise polynomials
- **High-order accurate spatial residual computation**:
  - Evaluation of interface hyperbolic flux
  - Accurate source term integration
- **Time Integration (evolve solution forward in time)**
  - Multi-stage explicit time marching schemes (e.g., RK2, RK4)

# CENO method

## Central Essentially Non-Oscillatory (CENO) Idea

- ENO Property: **Spurious oscillations** at points of discontinuity **are NOT allowed** (i.e. no Gibbs-like phenomenon ) but **they may exist** on the **order of truncation error**.
- Combine an unlimited $k$-exact reconstruction (Barth, 1993) with a monotonicity preserving limited linear ($k = 1$) scheme
- Hybrid method: use a solution smoothness indicator to switch between reconstruction procedures
- Use a single (central) stencil for reconstruction

**Note**: Harten & Chakravarthy (1991) explored ENO on fixed central stencil in 1D

$$TV(u^{n+1}) = TV(u^n) + O(\Delta x^{k+1})$$

UNIVERSITY OF WATERLOO

# piecewise-polynomial reconstruction

- Piecewise polynomial approximation for solution:

$$u^K_{i,j,\kappa}(\vec{r}) = \sum_{\substack{p_1=0 \\ (p_1+p_2+p_3 \le K)}}^{K} \sum_{p_2=0}^{K} \sum_{p_3=0}^{K} (x-\bar{x}_{i,j,\kappa})^{p_1} (y-\bar{y}_{i,j,\kappa})^{p_2} (z-\bar{z}_{i,j,\kappa})^{p_3} D_{p_1 p_2 p_3}$$

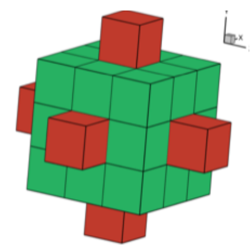

- Use a supporting stencil to determine coeffs $D_{p_1 p_2 p_3}$ (e.g., 20 and 35 unknowns for cubic and quartic reconstructions, respectively)
- Calculate $D_{p_1 p_2 p_3}$ by solving a least-squares problem for the conservation of mean solution, $\bar{u}_{i,j,k}$, in the supporting stencil

$$(\mathbb{A}\mathbf{D} - \mathbf{B})_{\gamma,\delta,\zeta} = \left( \frac{1}{V_{\gamma,\delta,\zeta}} \iiint_{\mathcal{V}_{\gamma,\delta,\zeta}} u^K_{i,j,k}(\vec{r})\, \mathrm{d}v \right) - \bar{u}_{\gamma,\delta,\zeta} = 0.$$

- Assess the local solution smoothness by comparing the predictions of the reconstructions that are part of the supporting stencil
- Revert reconstructions deemed as non-smooth to limited linear approx. **Note**: Each solution variable is individually assessed for smoothness

UNIVERSITY OF WATERLOO

# Gauss quadrature

- **More accurate calculation of flux and source term integrals**

$$\frac{1}{V_{i,j,k}} \oint_{\partial \mathcal{V}} \vec{\mathbf{F}} \cdot \vec{n}\, da = \frac{1}{V_{i,j,k}} \sum_{l=1}^{N_f} \sum_{m=1}^{N_G} \left( \omega \vec{\mathbf{F}} \cdot \vec{n}\, \Delta a \right)_{i,j,k,l,m}$$

$$\frac{1}{V_{i,j,k}} \iiint_{\mathcal{V}} (\mathbf{S} + \mathbf{Q})\, dv = \frac{1}{V_{i,j,k}} \sum_{v=1}^{N_V} (\omega (\mathbf{S} + \mathbf{Q}))_{i,j,k,v}$$

  - Use more Gauss quadrature points per face ($N_G \geq 4$)
  - Apply Gauss quadrature integration for general sources ($N_V \geq 8$)

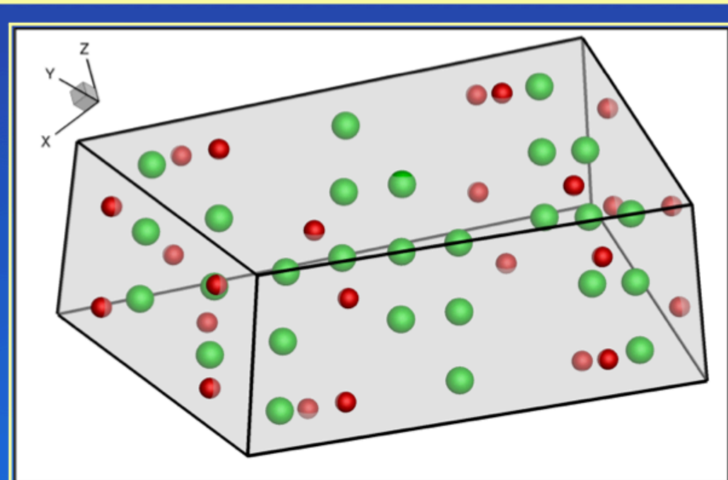

# smoothness indicator to decide on order of reconstruction

- Step 1: Calculate $\alpha$ (exploit the assumption of valid Taylor series expansion in the neighbourhood)

$$\alpha = 1 - \frac{\sum_{\gamma}\sum_{\delta}\sum_{\zeta}\left(u^K_{\gamma,\delta,\zeta}(\vec{\bar{r}}_{\gamma,\delta,\zeta}) - u^K_{i,j,\kappa}(\vec{\bar{r}}_{\gamma,\delta,\zeta})\right)^2}{\sum_{\gamma}\sum_{\delta}\sum_{\zeta}\left(u^K_{\gamma,\delta,\zeta}(\vec{\bar{r}}_{\gamma,\delta,\zeta}) - \bar{u}_{i,j,\kappa}\right)^2}$$

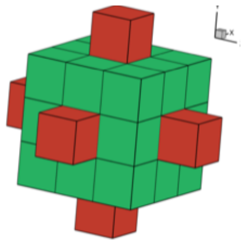

- Step 2: Evaluate $\mathcal{S}$ (inspired by the definition of multiple-correlation coefficients, Lawson, 1974)

$$\mathcal{S} = \frac{\alpha}{\max\left((1-\alpha),\epsilon\right)} \frac{(\mathcal{N}_{SOS} - \mathcal{N}_D)}{(\mathcal{N}_D - 1)}$$

$\mathcal{N}_{SOS}$ : Size of Stencil; $\mathcal{N}_D$ : Degrees of Freedom/Unknowns; $\epsilon = 10^{-8}$

$\alpha = 1$, $\mathcal{S}$ large: smooth flow

$\alpha < 1$, $\mathcal{S}$ small: discontinuous or under-resolved flow

# smoothness indicator

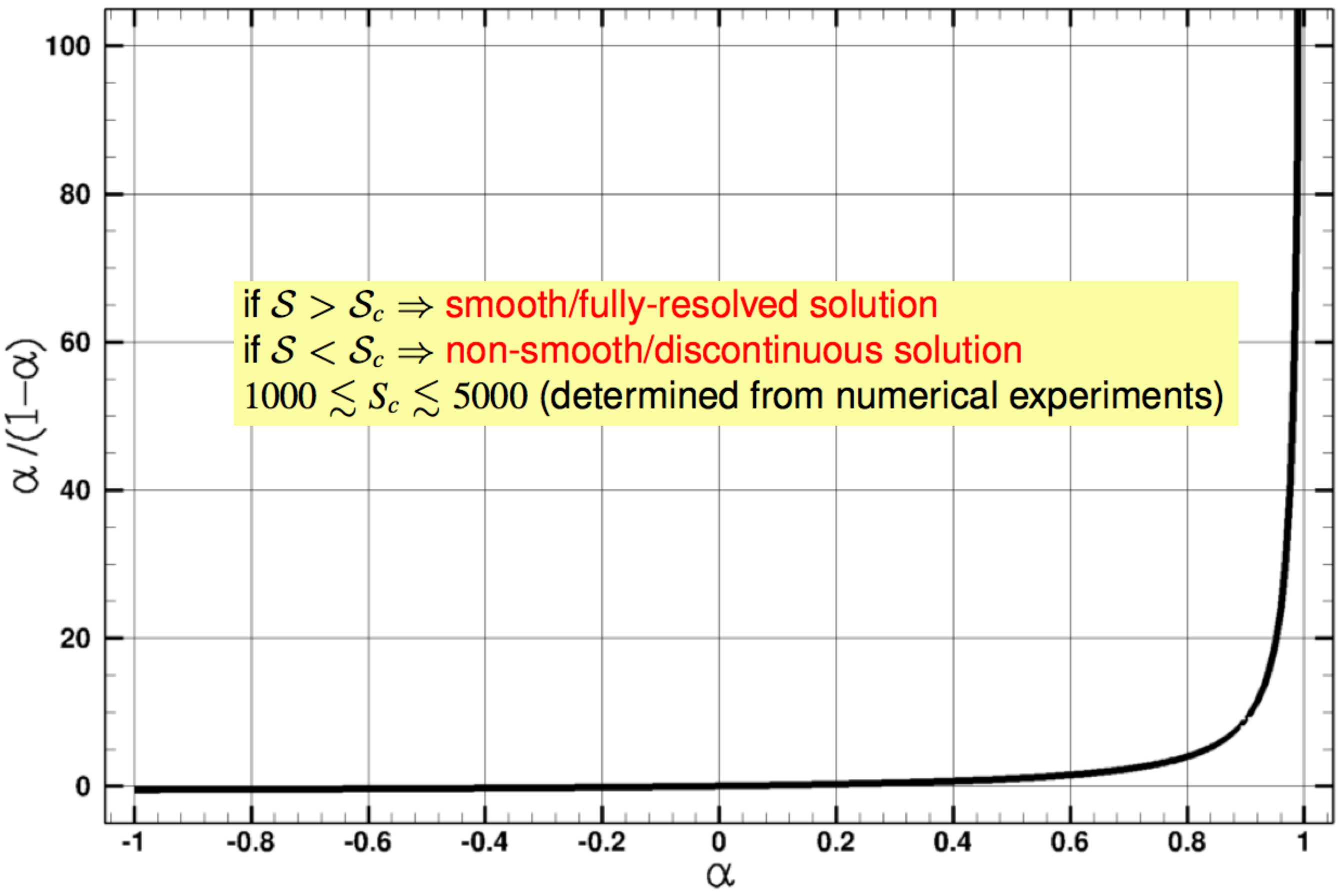


$\alpha$ = 1, $\mathcal{S}$ large: smooth flow

$\alpha$ <1, $\mathcal{S}$ small: discontinuous or under-resolved flow

# reconstruction stencils for cubic (*K*=3) reconstruction

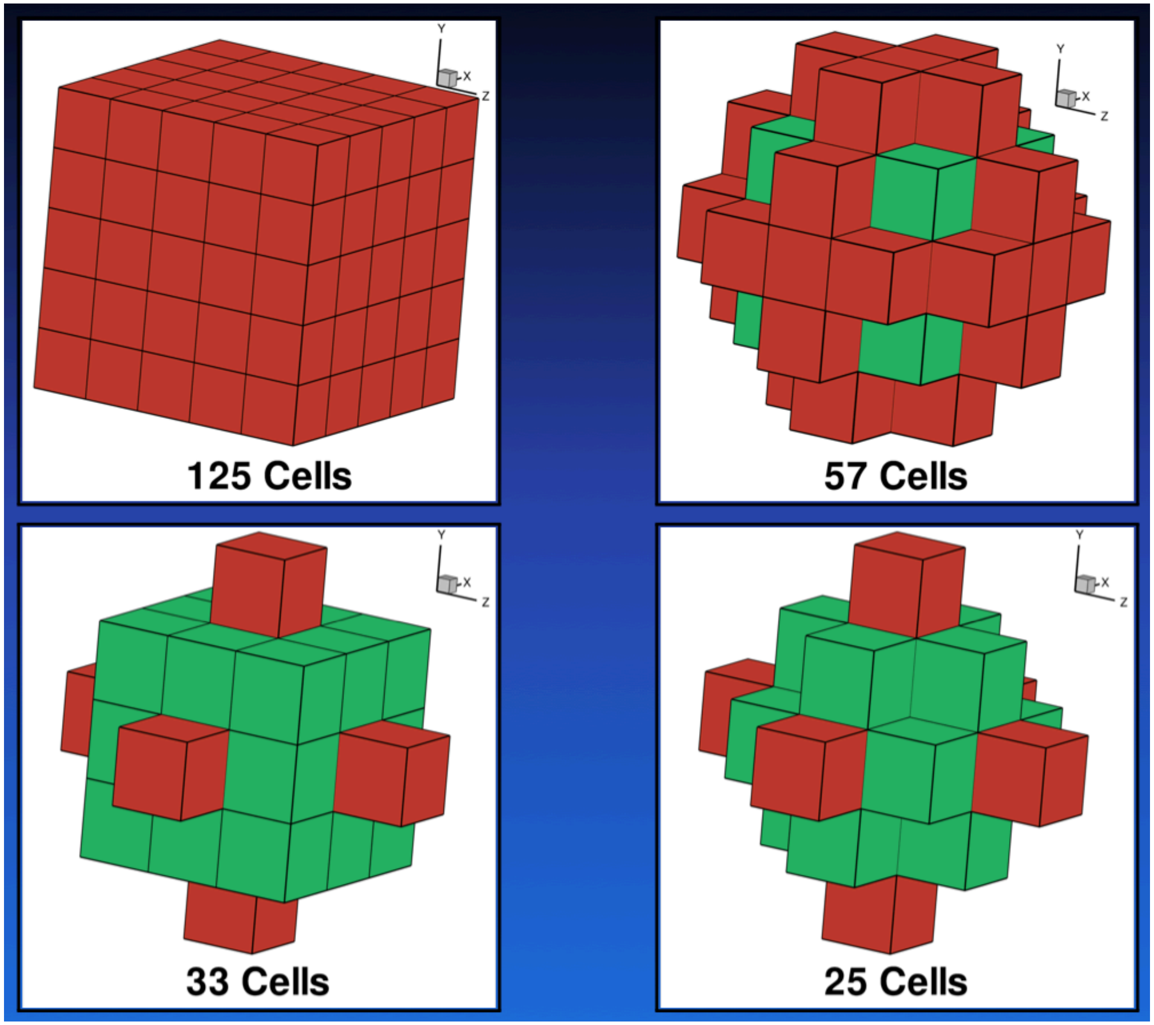

# 2D test problems

## superfast rotating outflow from cylinder

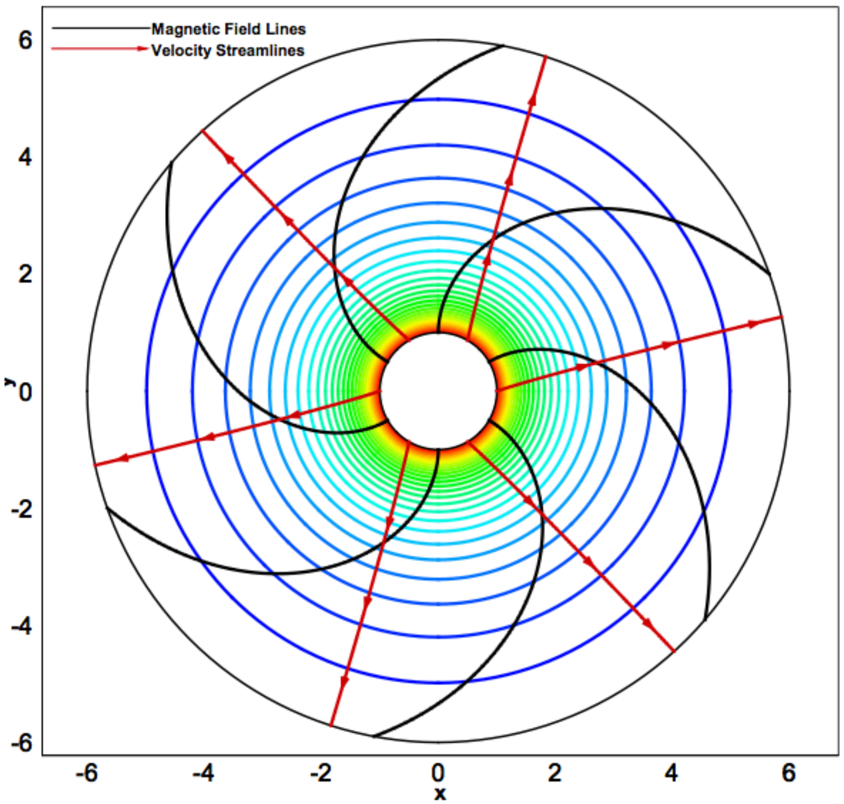


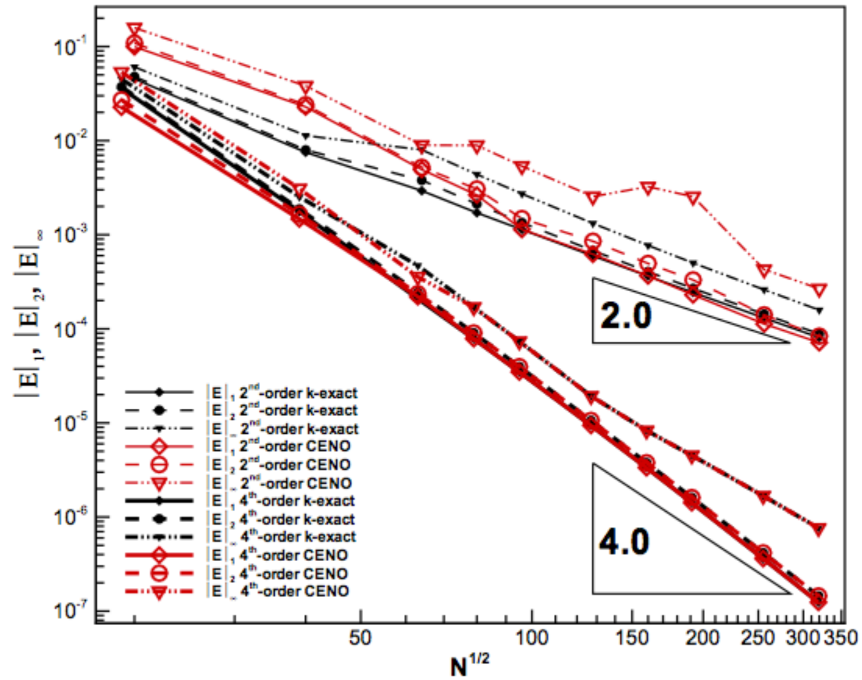


(a) The $L_1$-, $L_2$-, and $L_\infty$-norm errors for entropy, which is constant in the domain.

UNIVERSITY OF WATERLOO

# GLM handles $\nabla \cdot \vec{B}$ at grid resolution changes

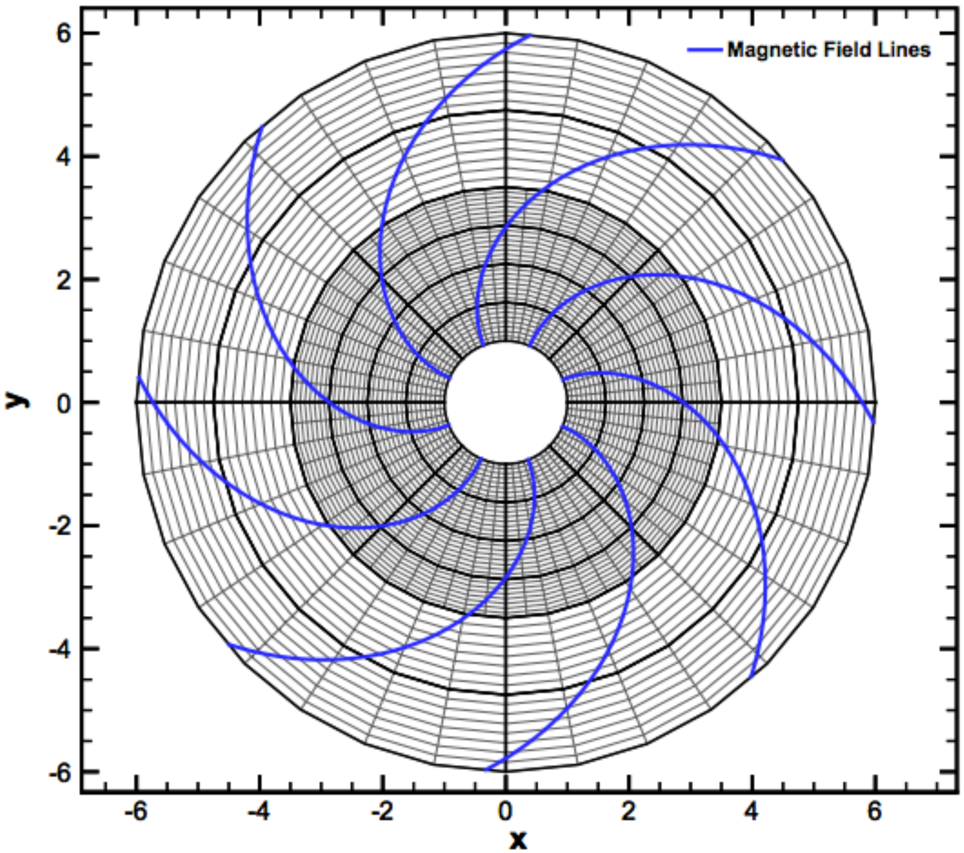


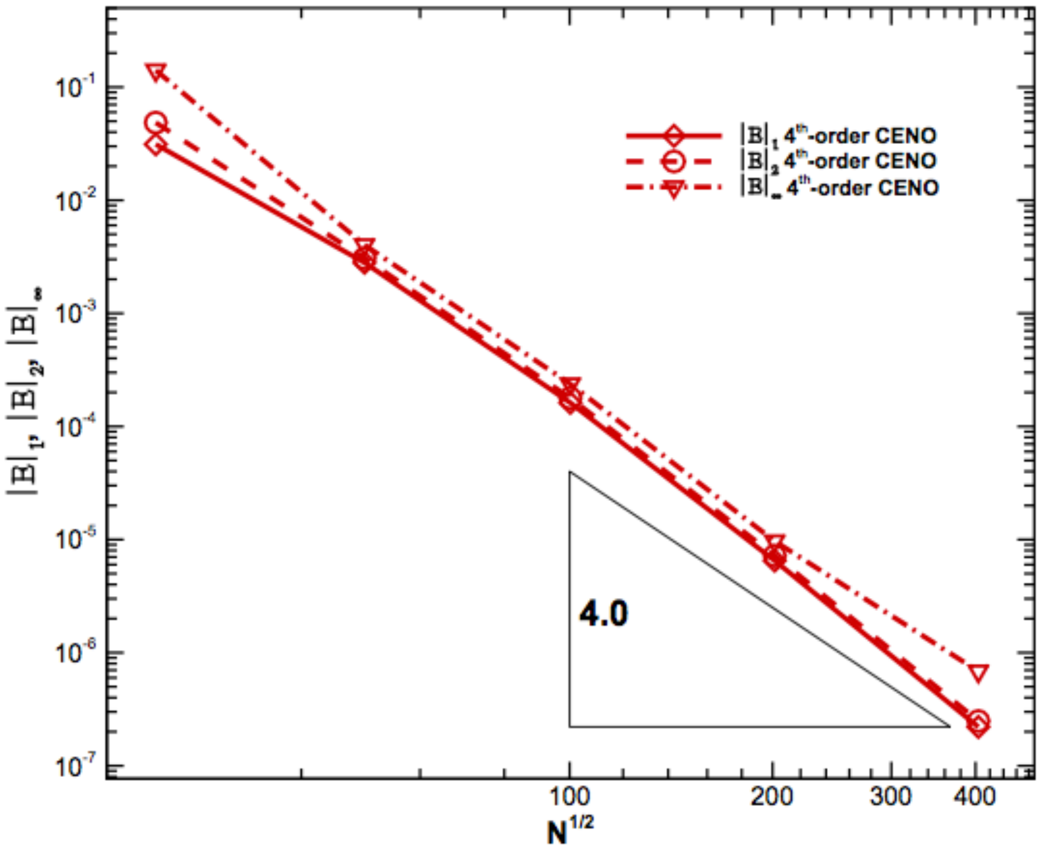


UNIVERSITY OF WATERLOO

# MHD version of Shu-Osher

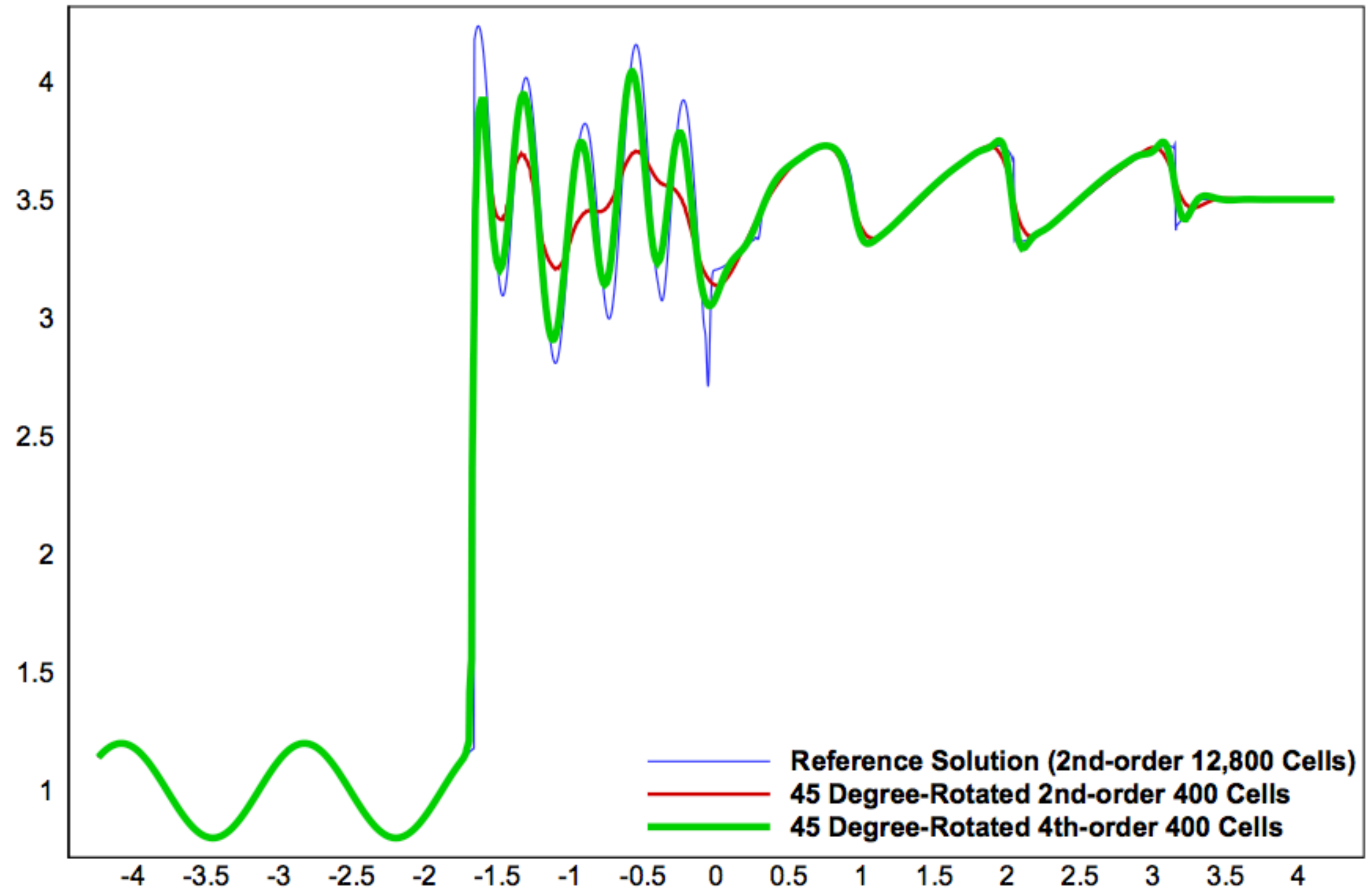


$$(\rho, u_\perp, u_\parallel, u_z, B_\perp, B_\parallel, B_z, p, \psi) = \begin{cases} (1,0,0,0,1,1,0,1,0) & \text{for } x < 4, \\ (3.5, 5.8846, 1.1198, 0, 1, 3.6359, 0, 42.0267, 0) & \text{for } x > 4 \end{cases}$$

$$\rho_l = 1 + 0.2\sin(5x), \quad \rho_r = 3.5$$

# dynamic adaptive refinement for Orszag-Tang vortex

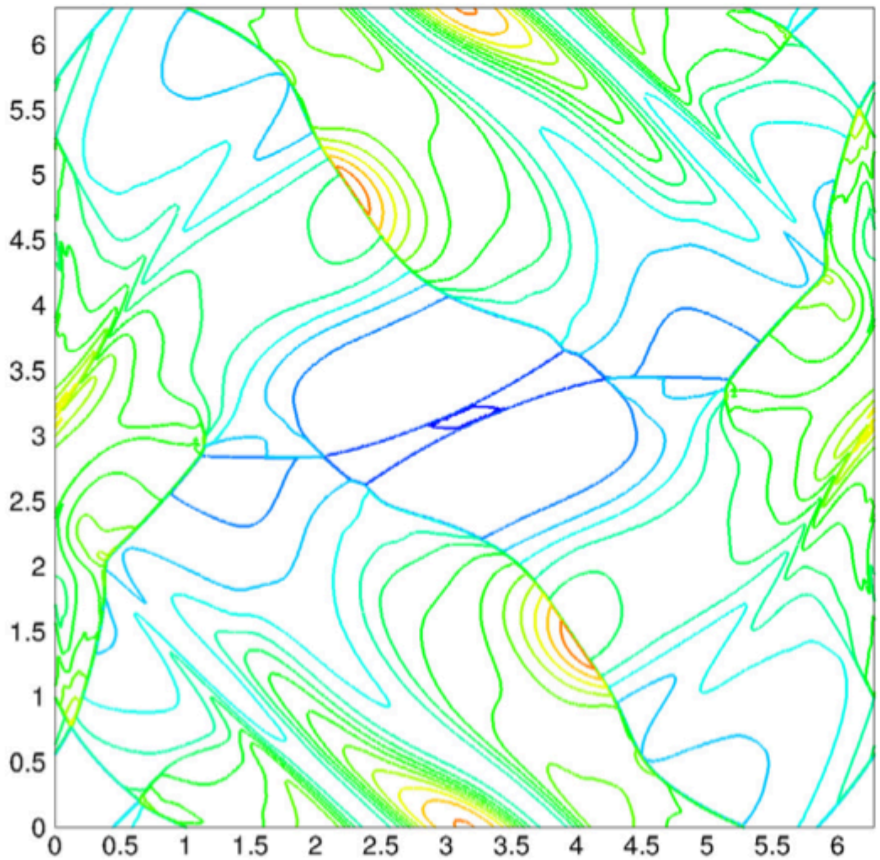


(c) Density solution at $t = 2.0$. The contour lines are equally spaced in the range (0.62,6.41) (15 contours).

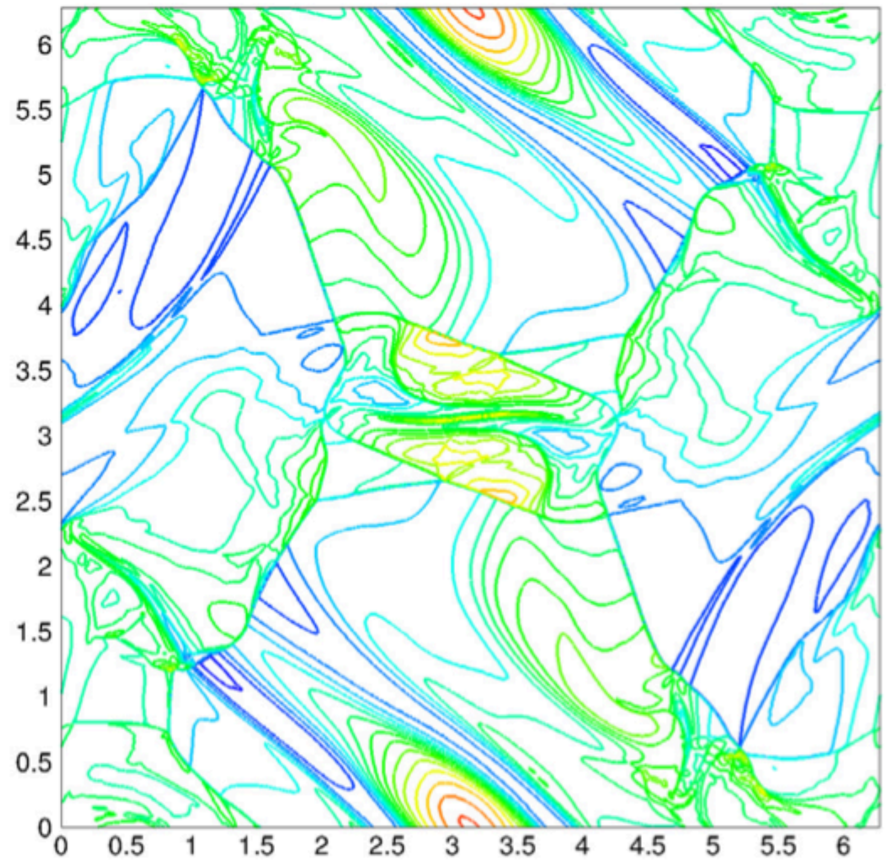


(d) Density solution at $t = 3.0$. The contour lines are equally spaced in the range (1.16,6.42) (15 contours).

$$v_x = -\sin(y),\ v_y = \sin(x),\ B_x = -\sin(y),\ B_y = \sin(2x)$$

UNIVERSITY OF WATERLOO

# dynamic adaptive refinement for Orszag-Tang vortex

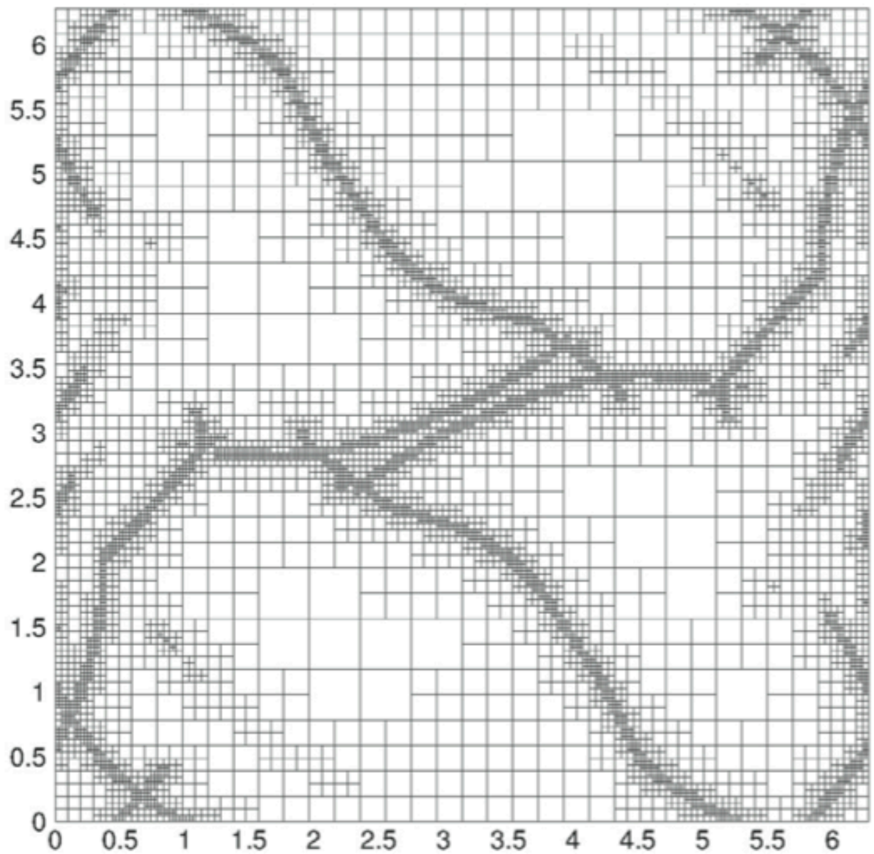


(c) AMR as applied to the Orszag-Tang vortex problem at $t =$ 2.0. At this point, the mesh consists of 8,428 8-by-8 blocks, or 539,136 cells in total.

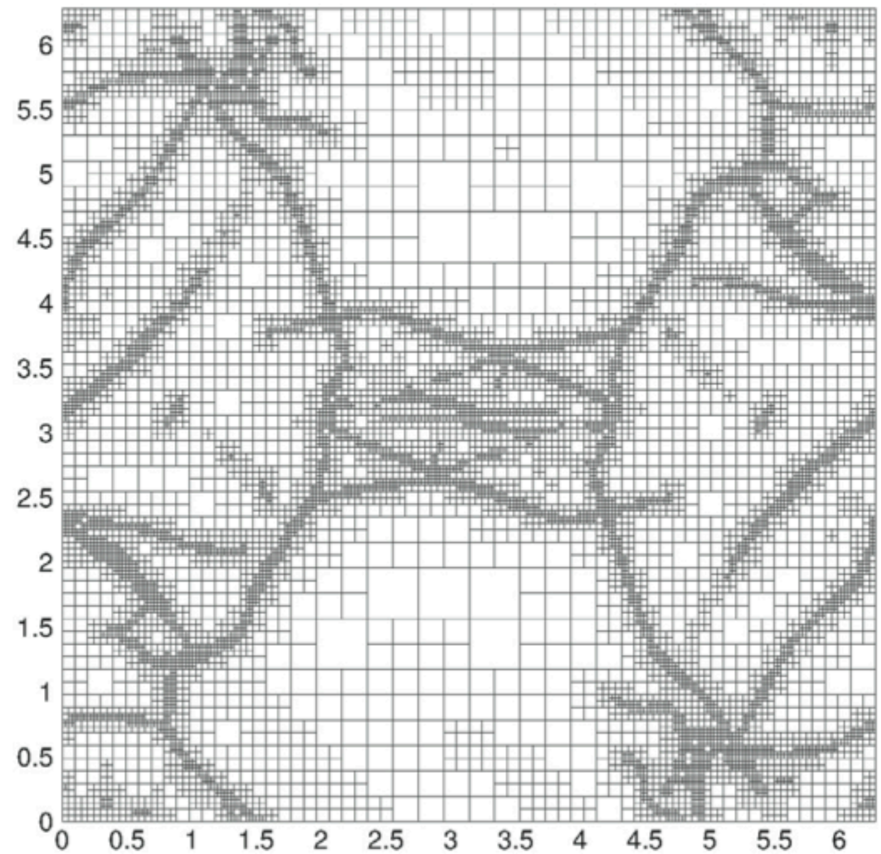


(d) AMR as applied to the Orszag-Tang vortex problem at $t =$ 3.0. At this point, the mesh consists of 13,522 8-by-8 blocks, or 865,408 cells in total.

# 2.4 adaptive cubed-sphere grids for space physics flows

- goal: solve PDE systems on a sphere (2D), or in a 3D domain between two concentric spheres
- cubed-sphere grids are attractive because
  - quasi-uniform (Cartesian panels)
  - no strong polar singularity

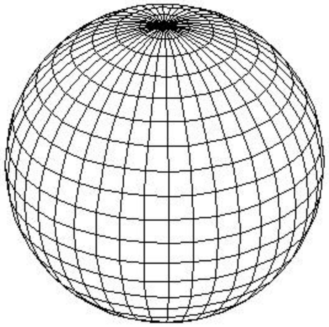

(image: mitgcm.org)

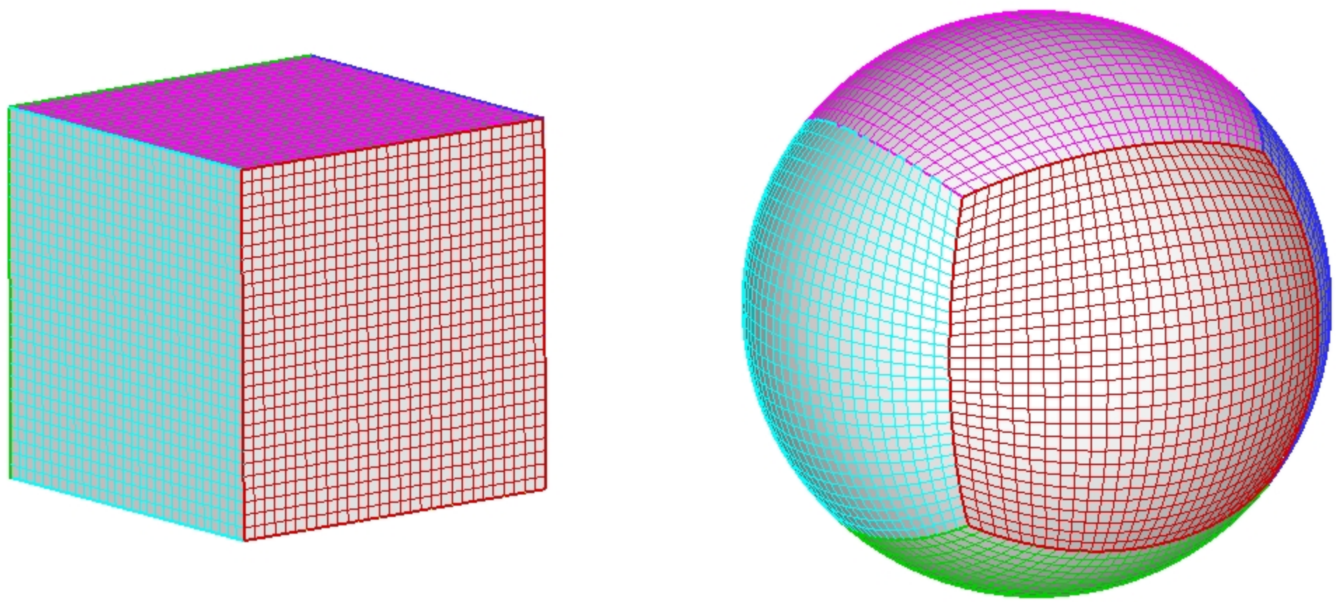

(image: Akshay Kulkarni (Harvard))

# cubed-sphere grids

- cubed-sphere grids are rapidly gaining popularity in a wide area of application fields (weather, climate, oceans, astrophysics, space physics, Earth mantle, ...)
- Sadourny, 1972; Ronchi et al., 1996; and many more authors since

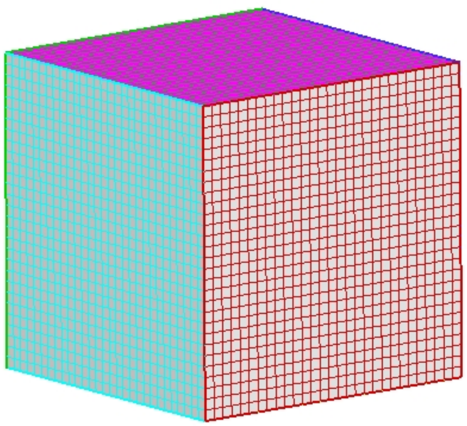

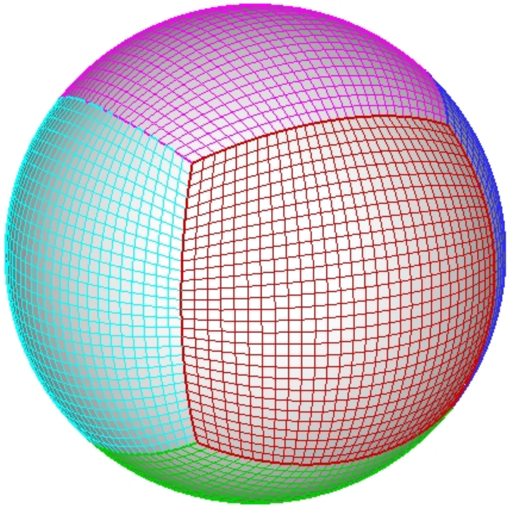

(image: Akshay Kulkarni (Harvard))

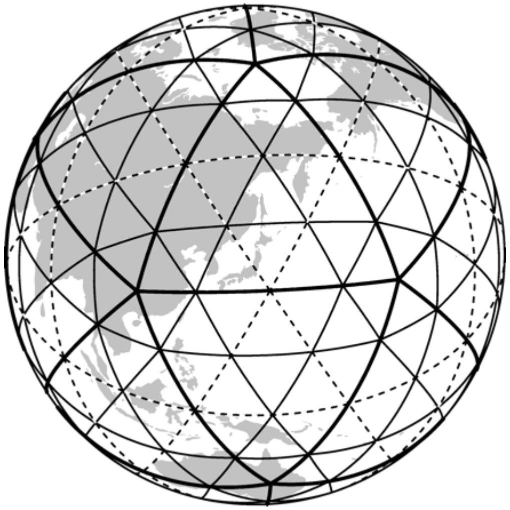

icosahedral grid
(image: Washington et al.)

# 3D cubed-sphere grids

- solve PDEs in domain between two concentric spheres
- 6 ‘sectors’ of the cubed-sphere grid (in 2D: panels)
- each sector is logically Cartesian
- sector boundaries and corners can cause difficulties

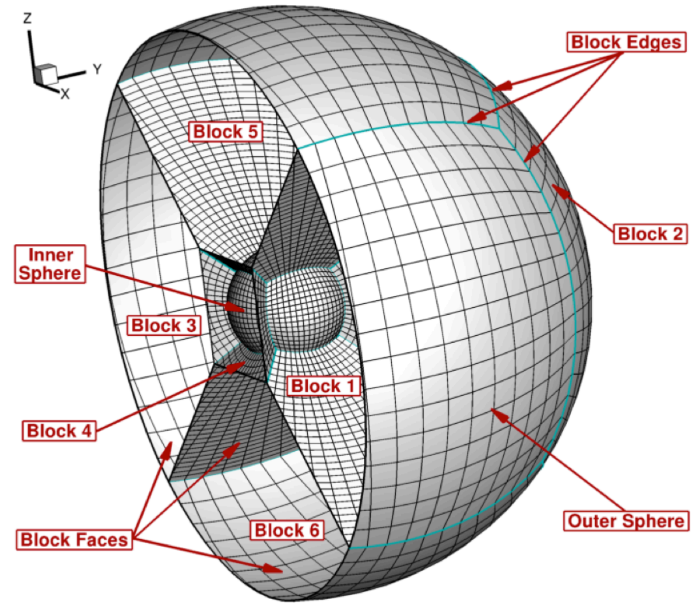


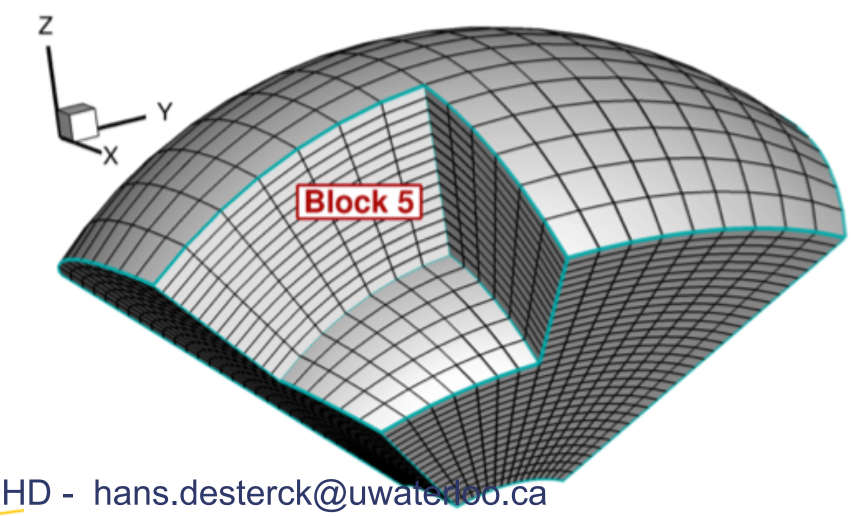

# our goals

- solve nonlinear hyperbolic conservation laws on 3D cubed-sphere grids, uniform 4th-order *accuracy*
- block-based *adaptive* grid refinement framework (logically Cartesian, self-similar blocks)
- large-scale *parallelism*: >30,000 adaptive blocks, >6,000 parallel CPU cores
- challenge: properly treat sector boundaries and corners

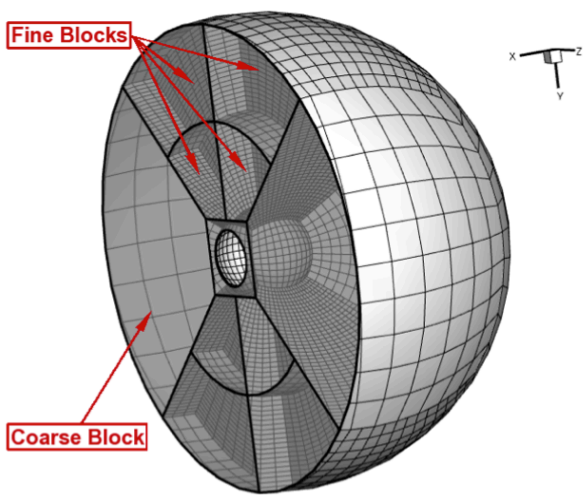


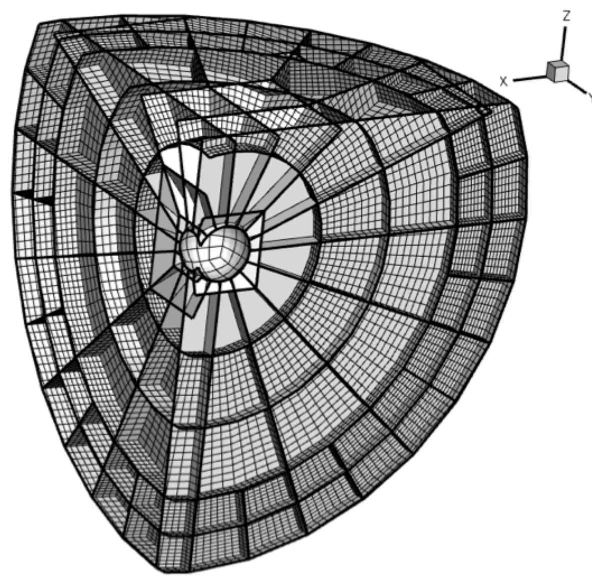

# our goals

- our application areas:
  - solar wind simulation (from Sun to Earth, 'Space Weather')
  - simulation of magnetic environments of Moon and Mars

➔ projects sponsored by the Canadian Space Agency ("Cluster for Lunar and Planetary Sciences: Advanced Coupled Models, Scientific Mission Definition, and Data Interpretation")

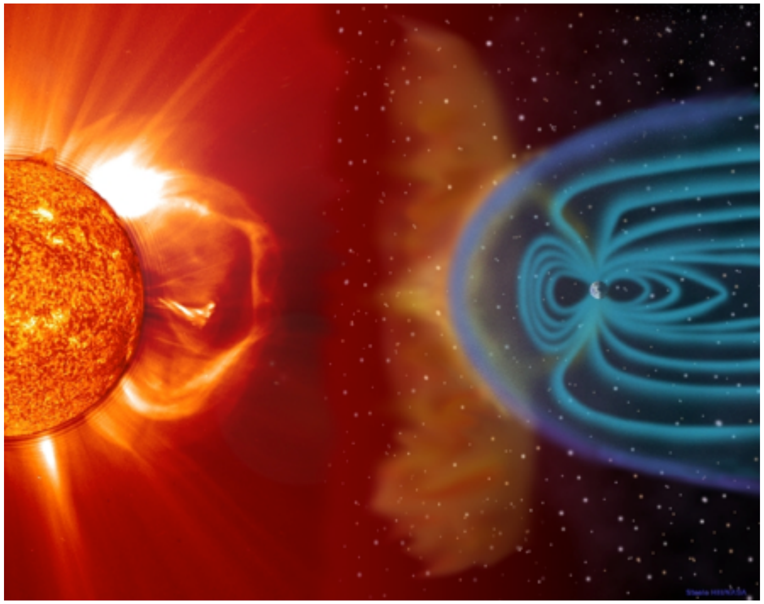

(image: SOHO/EIT consortium)

# our approach

1. use a fully multi-dimensional finite-volume discretization (not dimension-by-dimension)
   - least-squares based
   - can automatically handle varying stencil size (at sector corners)
   - at sector boundaries, can use cells from adjacent sectors directly, without need for special interpolation or reconstruction
   - maintains uniform 4th-order accuracy
   - discretization handles sector boundaries and corners in a ‘transparent’ (consistent, uniform) way (important for >30,000 adaptive blocks!)

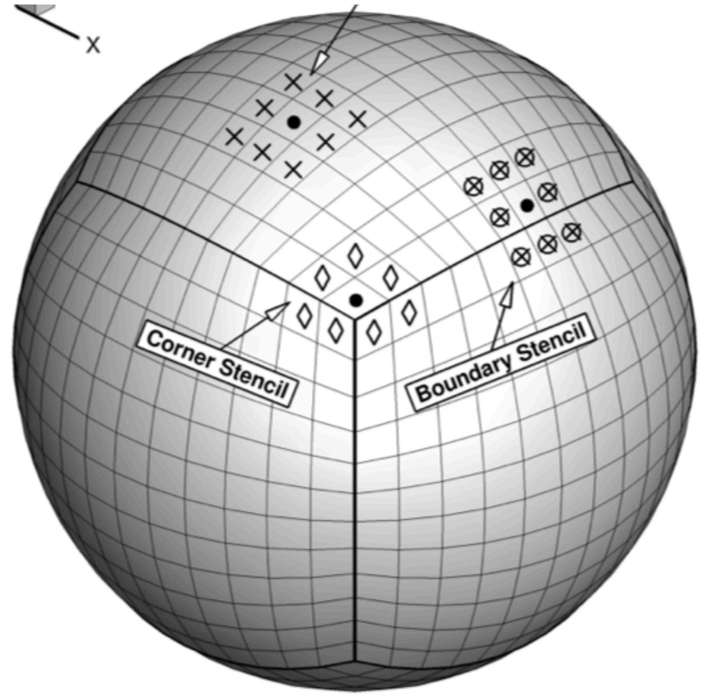


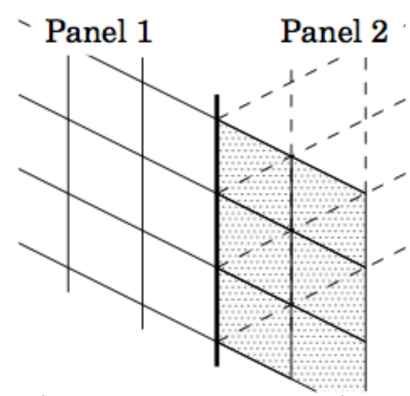


(image: Paul Ullrich)

# our approach

2. use multi-block approach where ‘all blocks are treated equally’
   - use sufficiently rich implementation concepts and data structures to make blocks ‘clever’ enough to handle sector boundaries and corners automatically/uniformly
   - sector boundaries and corners are treated ‘transparently’
   - this is a ‘software engineering’ CSE aspect, but it is crucial for managing code complexity if you want to do >30,000 adaptive blocks on >6,000 CPU cores

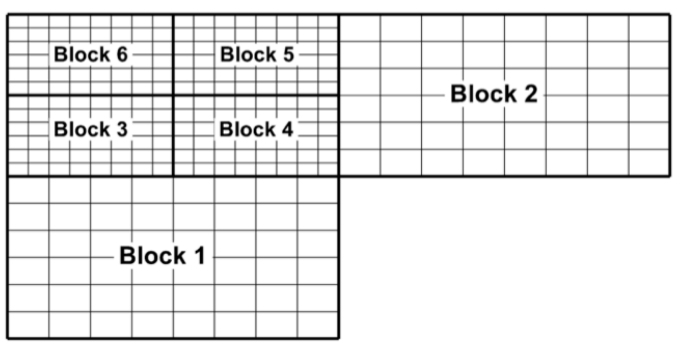


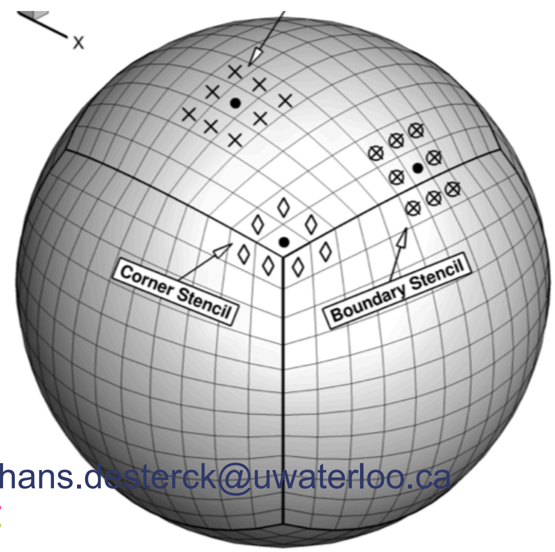


UNIVERSITY OF WATERLOO

# our approach

use multi-block approach where 'all blocks are treated equally'

in particular:

- multi-dimensional discretization
- multi-block code with unstructured root block connectivity
- consistently keep track of *(i,j,k)* orientation and ordering of adjacent blocks (we use 'Computational Fluid Dynamics General Notation System' (CGNS))

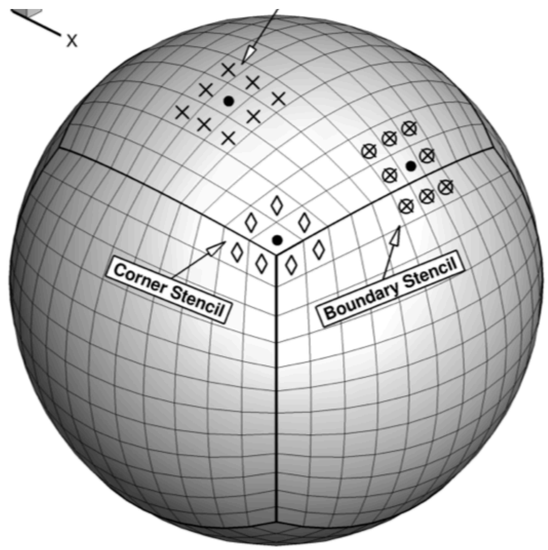


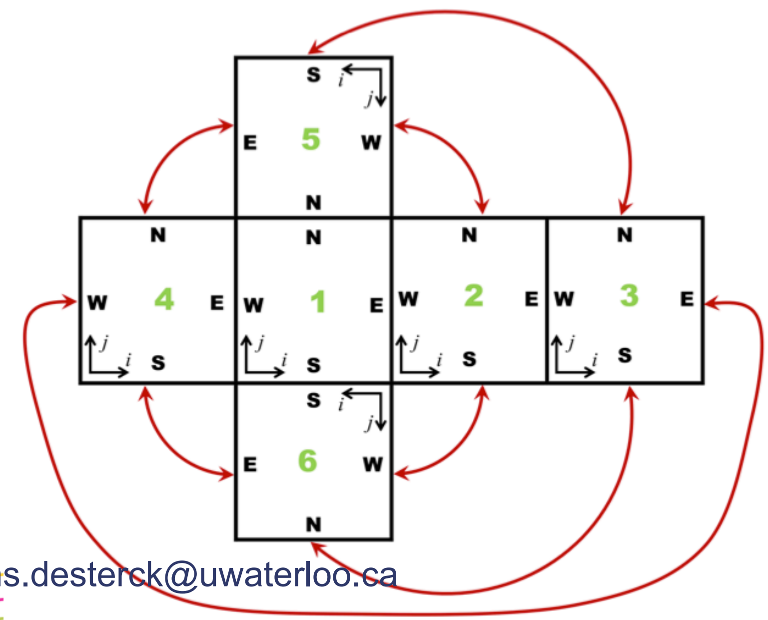


UNIVERSITY OF WATERLOO

# our contributions

- L. Ivan, H. De Sterck, S. Northrup, and C. Groth, ‘Three-Dimensional MHD on Cubed-Sphere Grids: Parallel Solution-Adaptive Simulation Framework’, **AIAA CFD Conference, 2011, AIAA paper 2011-3382**
- Lucian Ivan, Hans De Sterck, Scott A. Northrup, and Clinton P. T. Groth, ‘Multi-Dimensional Finite-Volume Scheme for Hyperbolic Conservation Laws on Three-Dimensional Solution-Adaptive Cubed-Sphere Grids’, **Journal of Computational Physics, accepted, 2013**
- L. Ivan, A. Susanto, H. De Sterck, and C. Groth, ‘High-Order Central ENO Finite-Volume Scheme for MHD on Three-Dimensional Cubed-Sphere Grids’, **Seventh International Conference on Computational Fluid Dynamics (ICCFD7), 2012**

# block-based adaptive grid framework

- use self-similar, logically Cartesian blocks (e.g., 8x8x8)
- use octree data structure with six root blocks
- implemented in C++, templated
- the same framework is also used/developed in Groth's group for combustion simulations (Groth's CFFC framework was starting point for our work) (Gao and Groth, 2010)

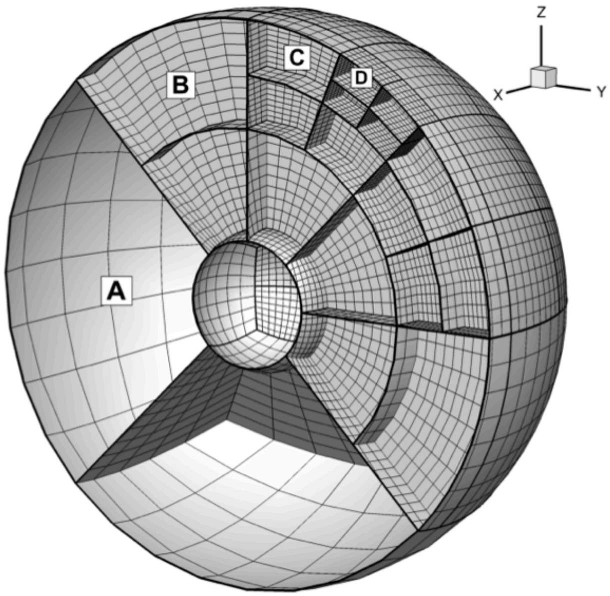


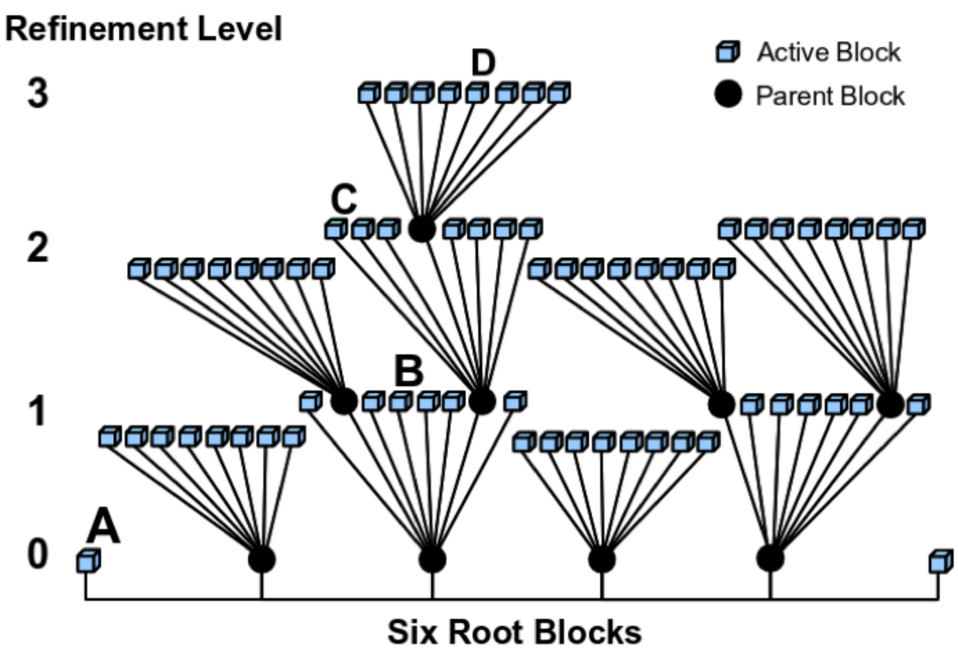

# adaptive grid refinement

- adaptive refinement (1→8 blocks) and coarsening (8→1 block)
- physics-based refinement criteria (e.g., density gradient)
- dynamic refinement and coarsening (refinement follows moving features)

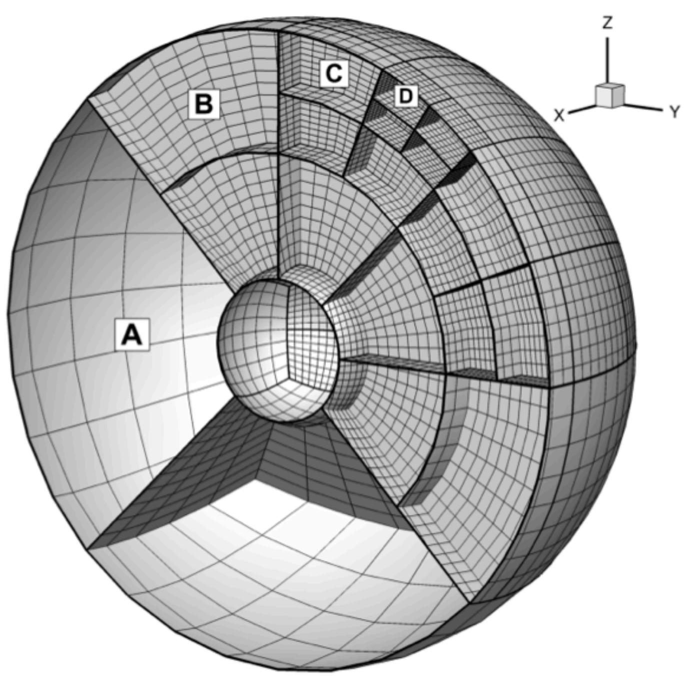


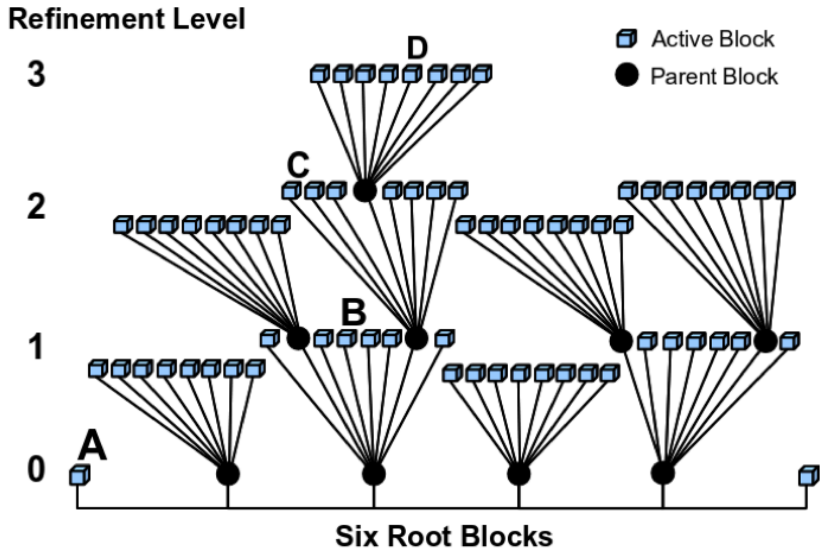

# adaptive grid refinement

- adjacent blocks cannot differ in resolution by more than a factor of two
- implementation for cubed-sphere greatly facilitated by ‘all blocks are treated equally’ (dynamic refinement!)

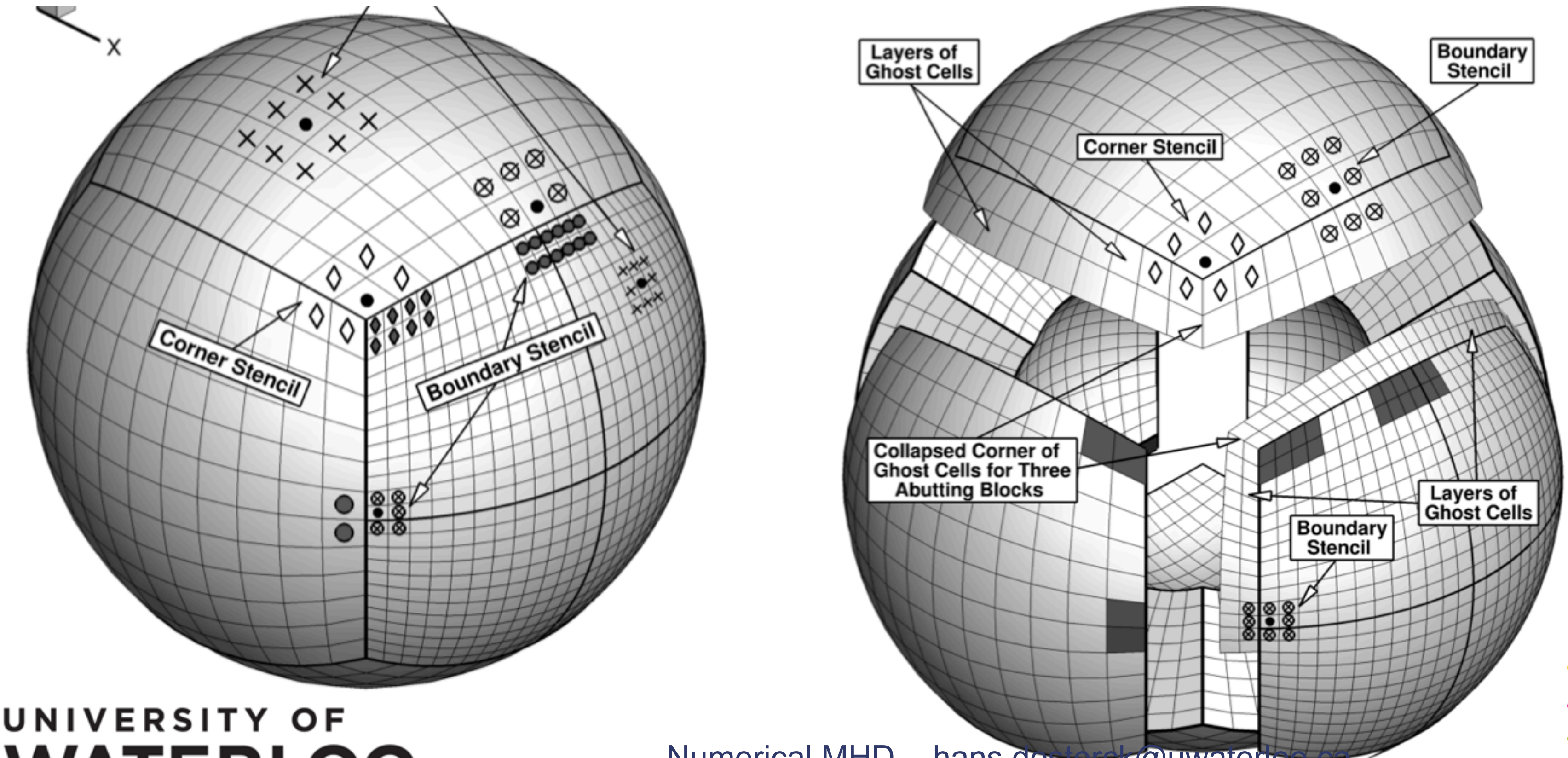

# high-order challenge 1: non-planar cell surfaces

$$\boxed{\partial_t \mathbf{U} + \vec{\nabla} \cdot \vec{\mathbf{F}} = \mathbf{S} + \mathbf{Q}}$$

$$\frac{d\overline{\mathbf{U}}_{ijk}}{dt} = -\frac{1}{V_{ijk}} \sum_{f=1}^{6} \sum_{m=1}^{N_g} \left(\tilde{\omega} \vec{\mathbf{F}}_{\mathrm{num}} \cdot \vec{n}\right)_{i,j,k,f,m} + \left(\overline{\mathbf{S}}\right)_{ijk} + \left(\overline{\mathbf{Q}}\right)_{ijk} = \mathbf{R}_{ijk}(\overline{\mathbf{U}})$$

- Piecewise polynomial approximation for solution:

$$u^{K}_{i,j,\kappa}(\vec{r}) = \underset{(p_1+p_2+p_3 \le K)}{\sum_{p_1=0}^{K} \sum_{p_2=0}^{K} \sum_{p_3=0}^{K}} (x - \bar{x}_{i,j,\kappa})^{p_1} (y - \bar{y}_{i,j,\kappa})^{p_2} (z - \bar{z}_{i,j,\kappa})^{p_3} D_{p_1 p_2 p_3}$$

- Use a trilinear interpolation to represent skewed hexas accurately
- Compute geometric properties (e.g., volume, centroid, normals, geometric moments) using the trilinear mapping
- Integrate fluxes appropriately (4 points per face for a 4th-order scheme)

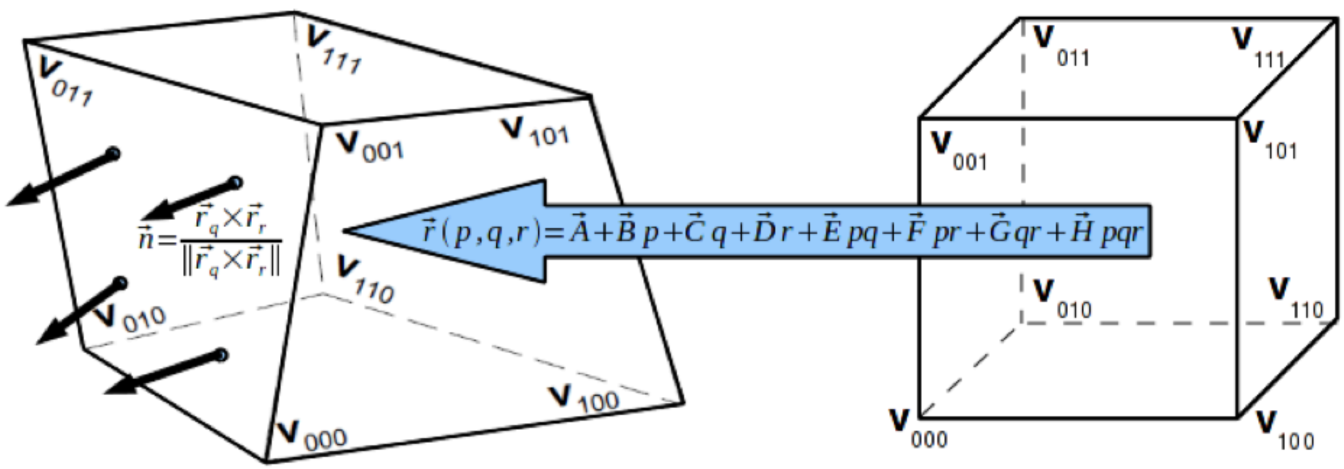


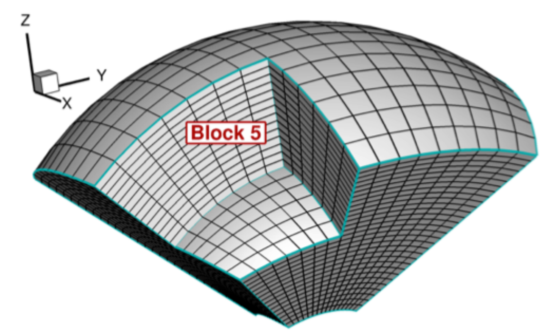


UNIVERSITY OF WATERLOO

# high-order challenge 2: degenerate stencils at sector edges and corners (rotation mechanism)

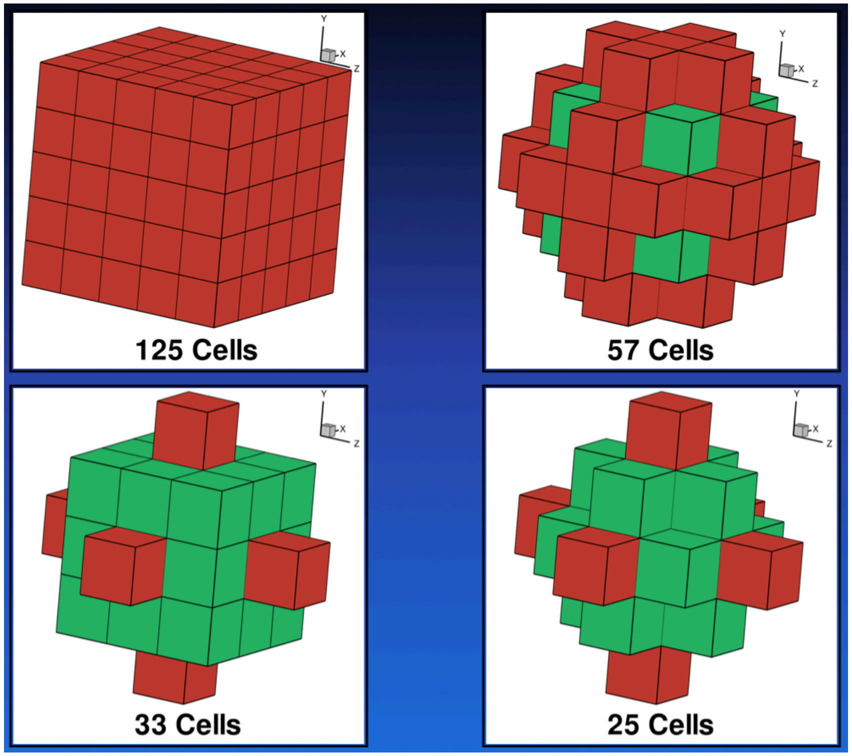


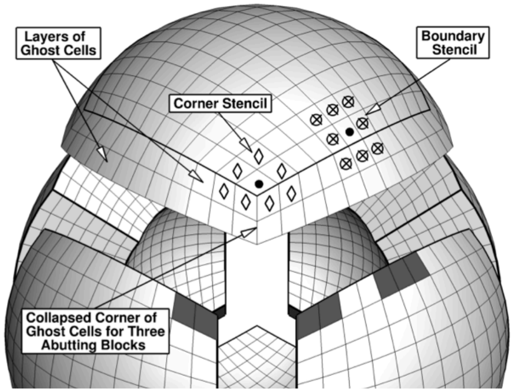


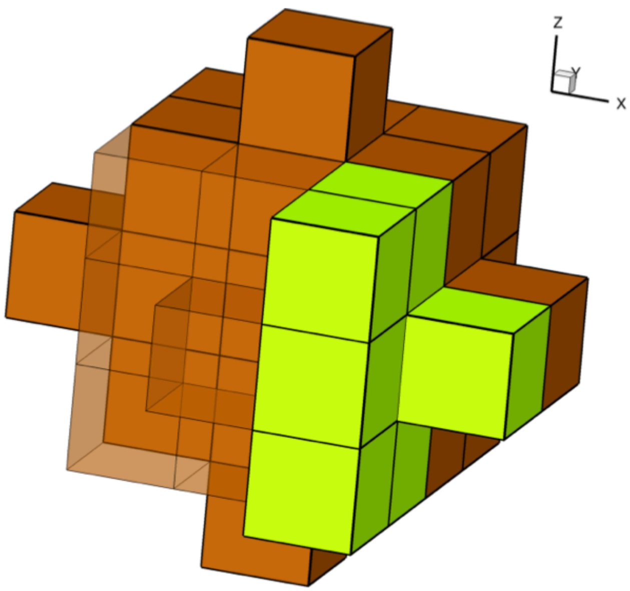

# parallelisation

- two (or more) layers of ghost cells for each block
- MPI message passing

- many more blocks than processors
- self-similar blocks: load-balancing by equally distributing blocks over CPU cores (Morton ordering can be employed)

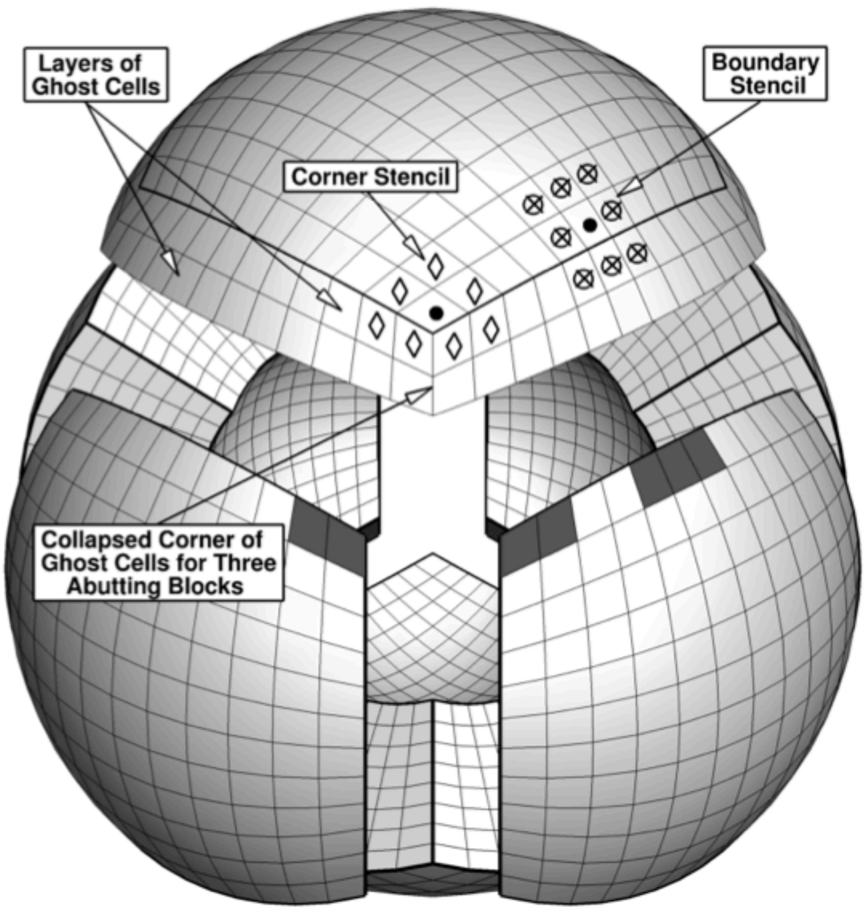

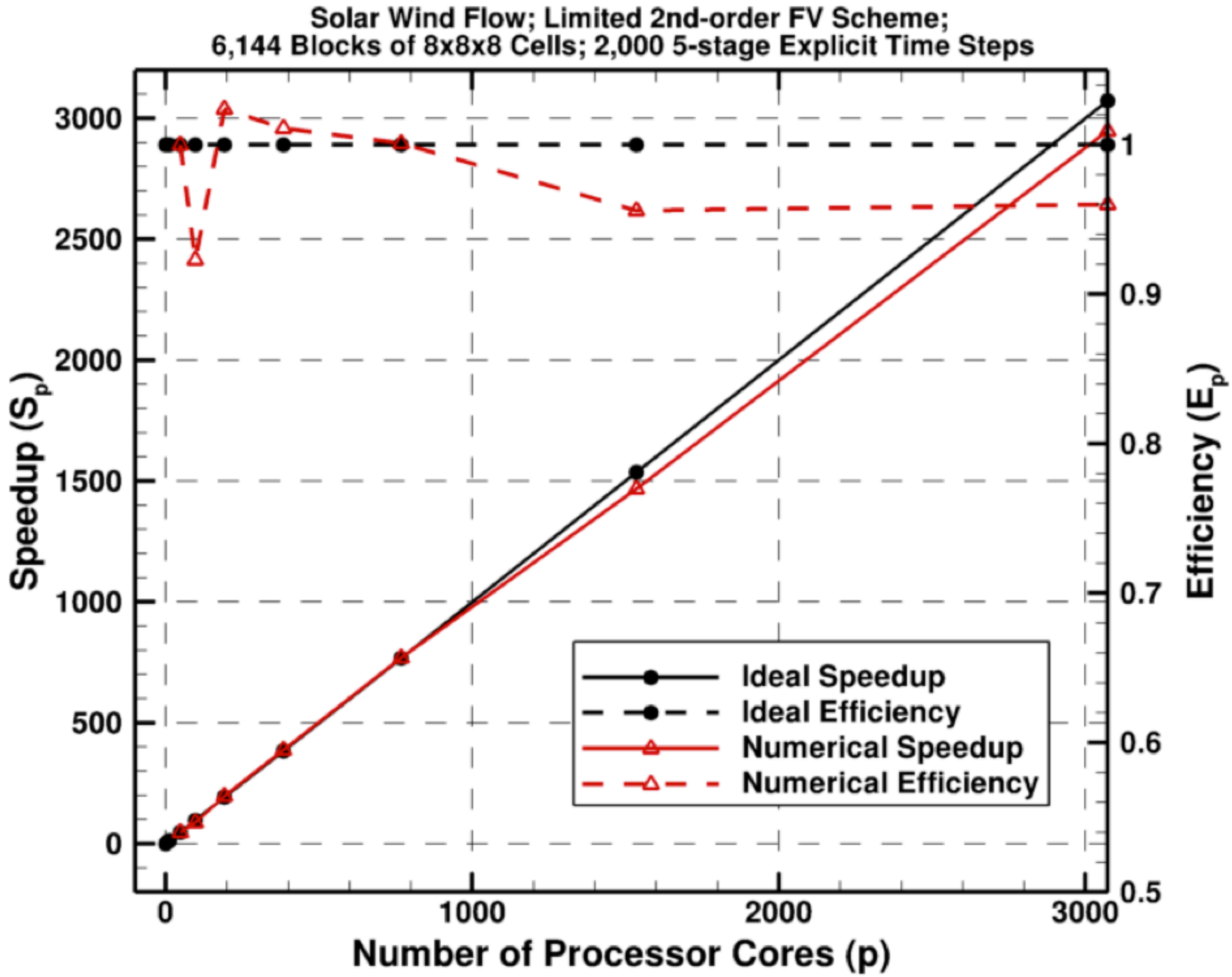


UNIVERSITY OF WATERLOO

# validation tests

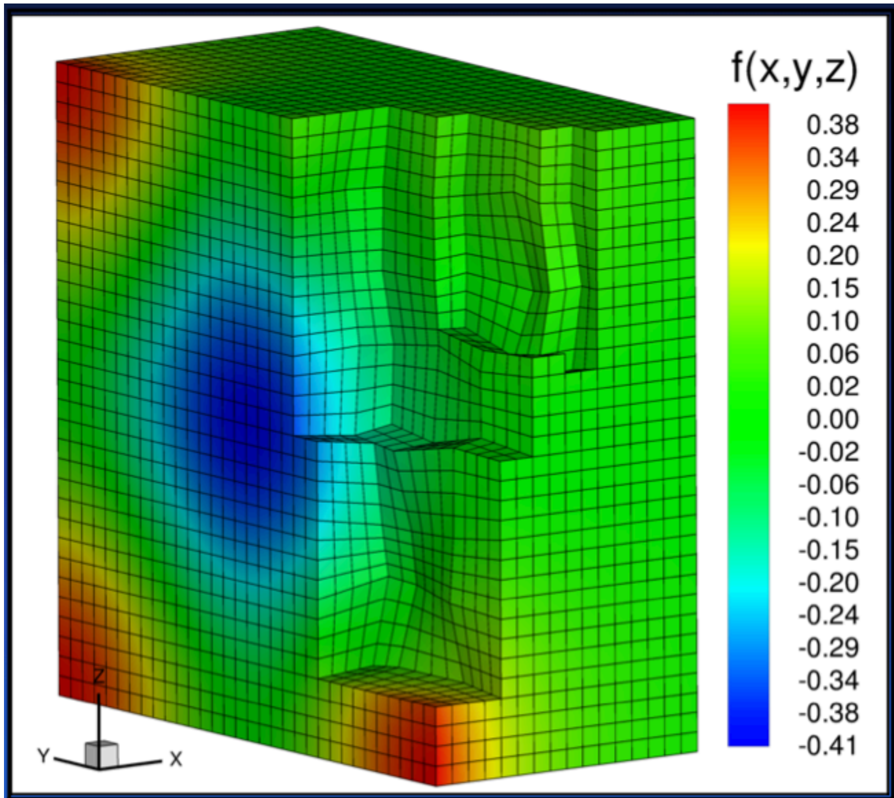


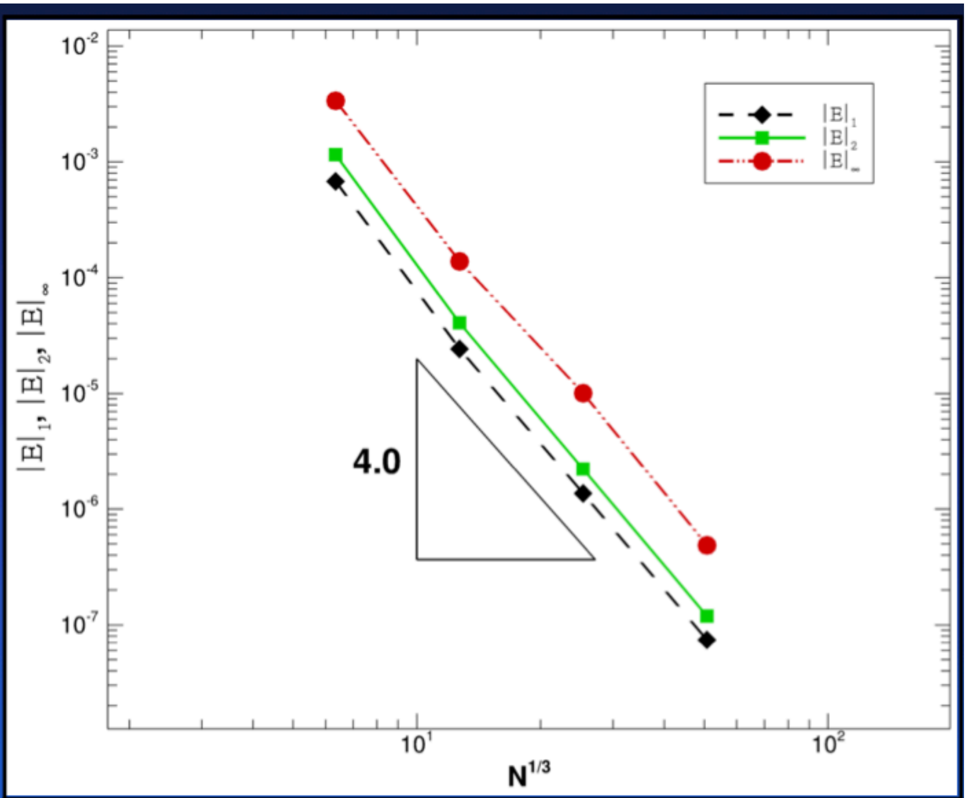


Solution reconstruction obtained using the **4th-order CENO** scheme on a mesh with 8 blocks of $4 \times 8 \times 8$ and 2,048 cells (left) and error norms (right).

# validation tests

**Magnetohydrostatic Test Case on Cartesian Box (Warburton 1999)**

$$\mathbf{U}(x,y,z)=\left[1,\vec{0},\,(\cos(\pi(y+1))-\cos(\pi z))f(x),\,\cos(\pi z)f(y)+\sin(\pi(y+1))f(x),\,\sin(\pi z)(f(y)-f(x)),\,5+0.5\left(B^2{}_x+B^2{}_y+B^2{}_z\right)\right]^T$$

$$f(u)=e^{-\pi(u+1)}$$

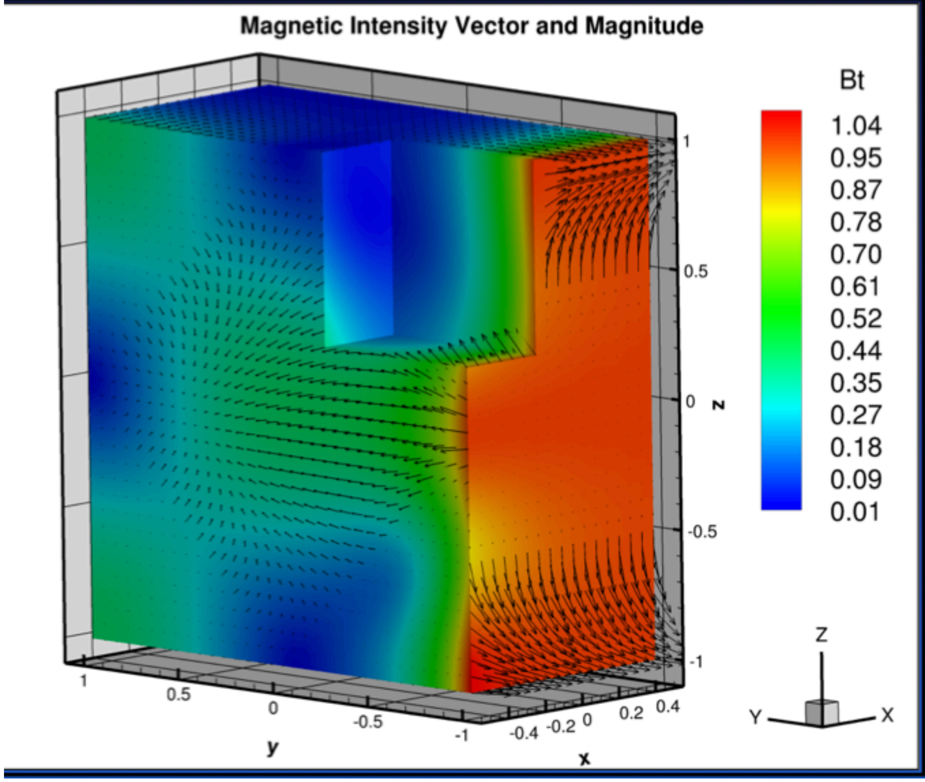


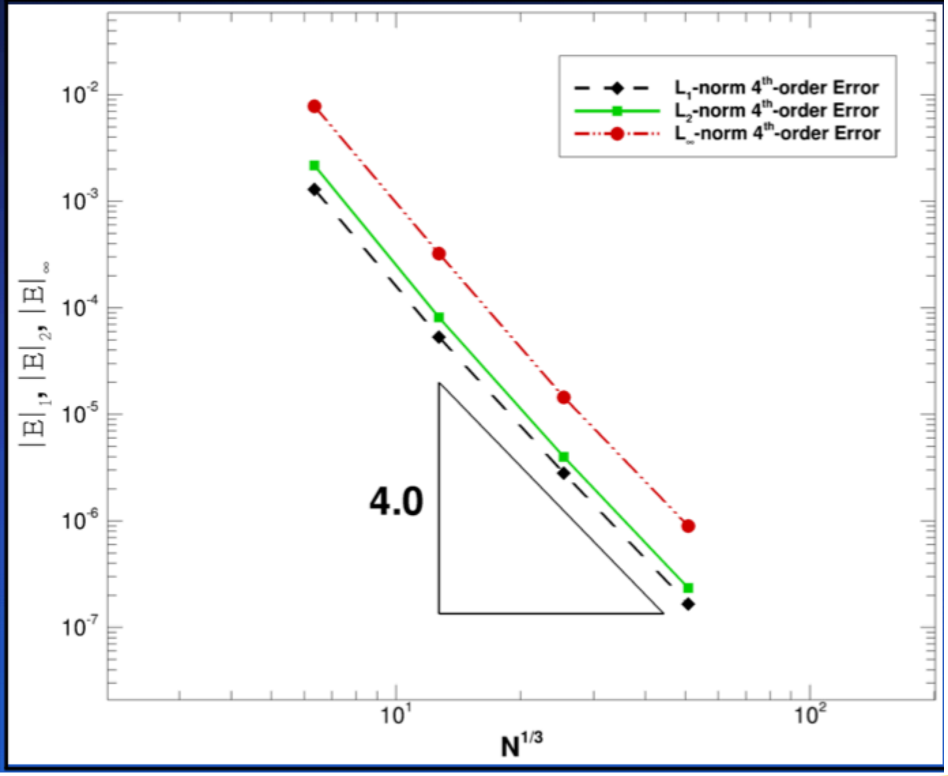

# validation tests

**Solution to Manufactured Problem** $R_i = 2$, $R_o = 3.5$, $M_{cf} > 0$ **everywhere**

$$\mathbf{U}(x,y,z) = \left[\; r^{-\frac{5}{2}},\ \frac{x}{\sqrt{r}},\ \frac{y}{\sqrt{r}},\ \frac{z}{\sqrt{r}} + \kappa r^{\frac{5}{2}},\ \frac{x}{r^3},\ \frac{y}{r^3},\ \frac{z}{r^3} + \kappa,\ r^{-\frac{5}{2}} \;\right]^T, \quad \kappa = 0.017$$

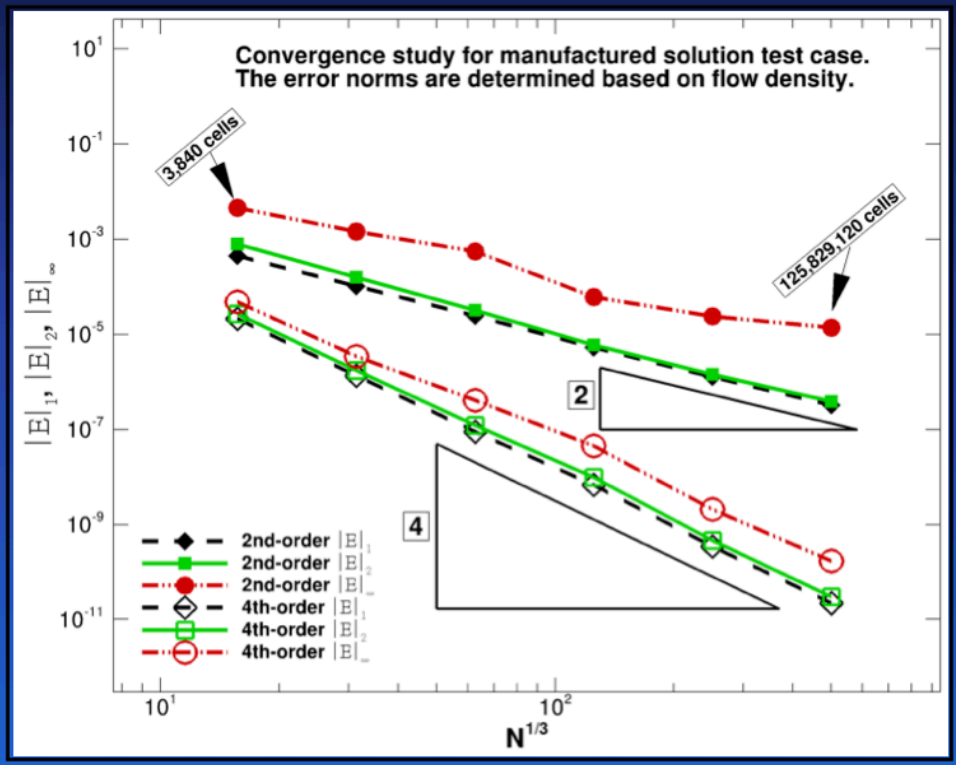


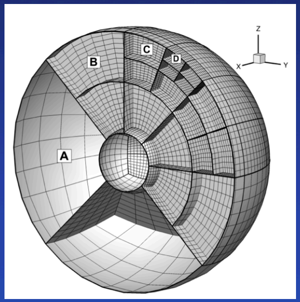

# large-scale results

- ‘magnetically dominated’ MHD bow shock flow (2nd-order)
- we only use 5 root blocks
- 7 refinement levels with 22,693 blocks and 14,523,520 computational cells

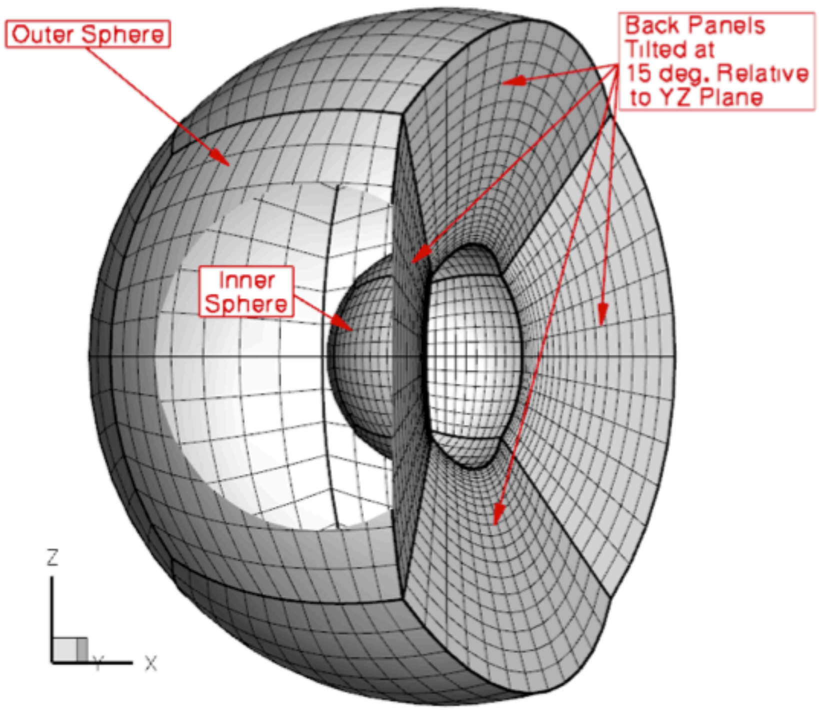


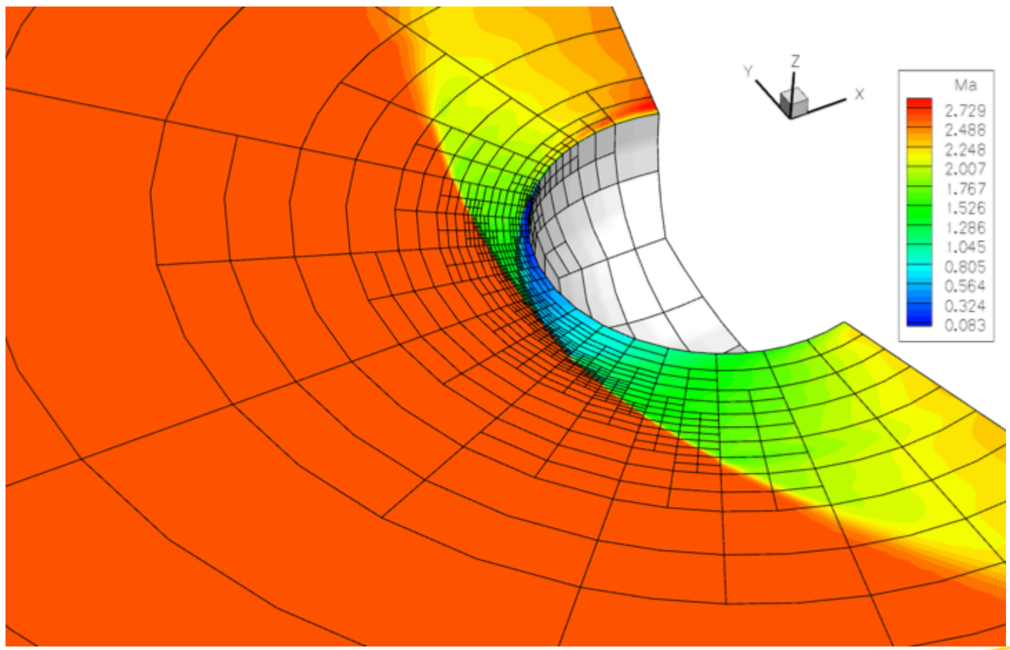

# large-scale results

- MHD solar wind (Groth et al. model) ($2^{nd}$-order)

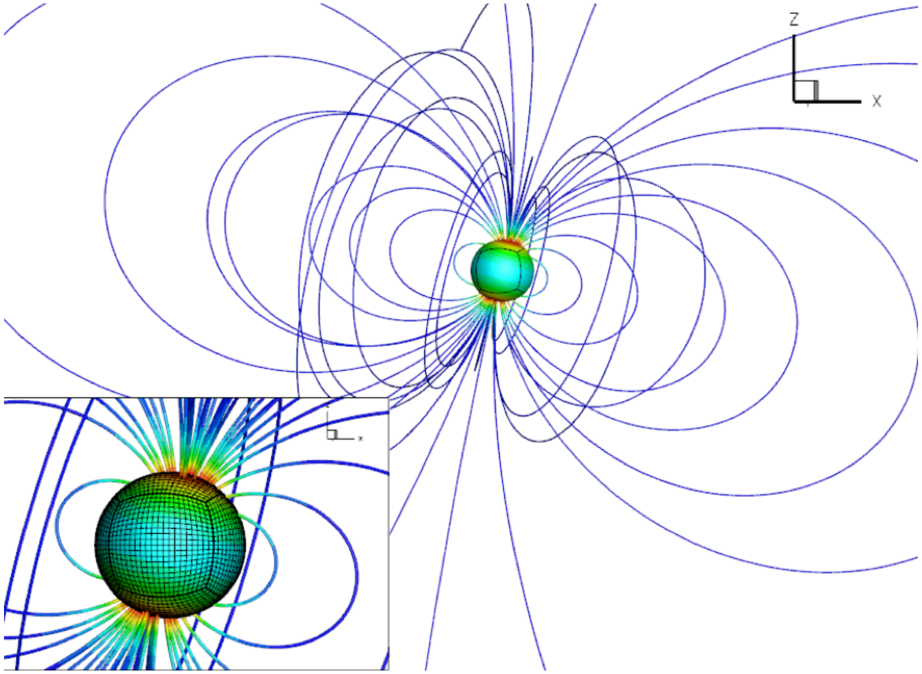


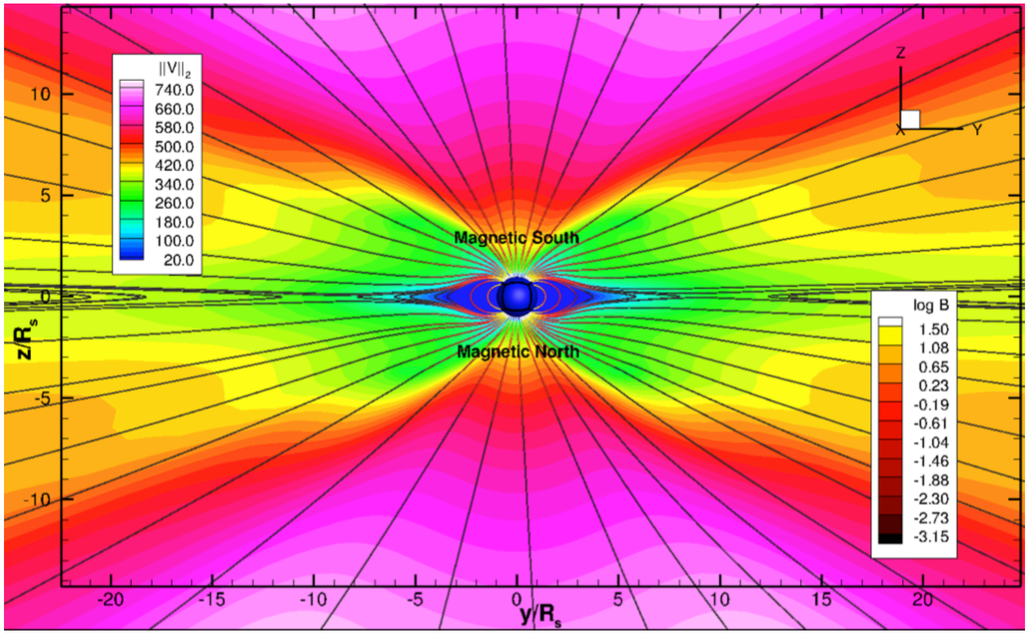

# large-scale results

- MHD solar wind (Groth et al. model)

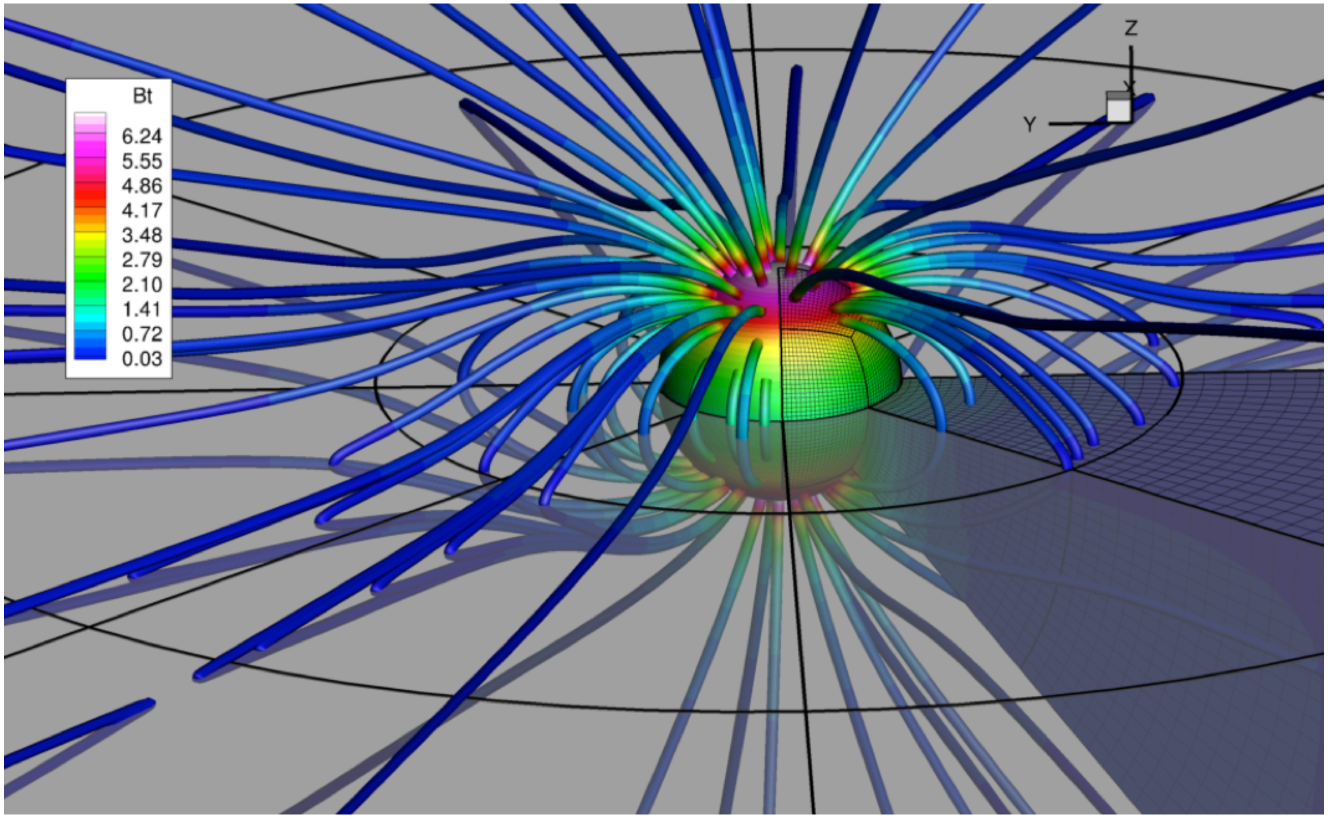

# ongoing and future work

- Mars/Moon simulations (need to solve PDE inside the spherical object ➔ 7 root blocks!)

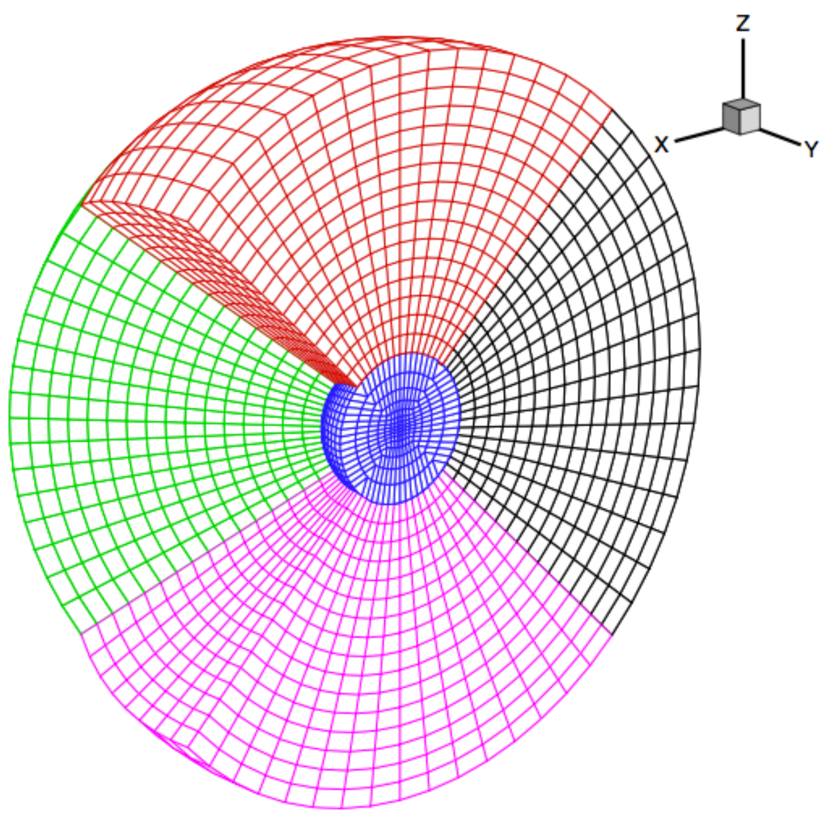


UNIVERSITY OF WATERLOO

# ongoing and future work

- our framework is flexible enough to handle multiple spherical objects (e.g., Earth and Moon)

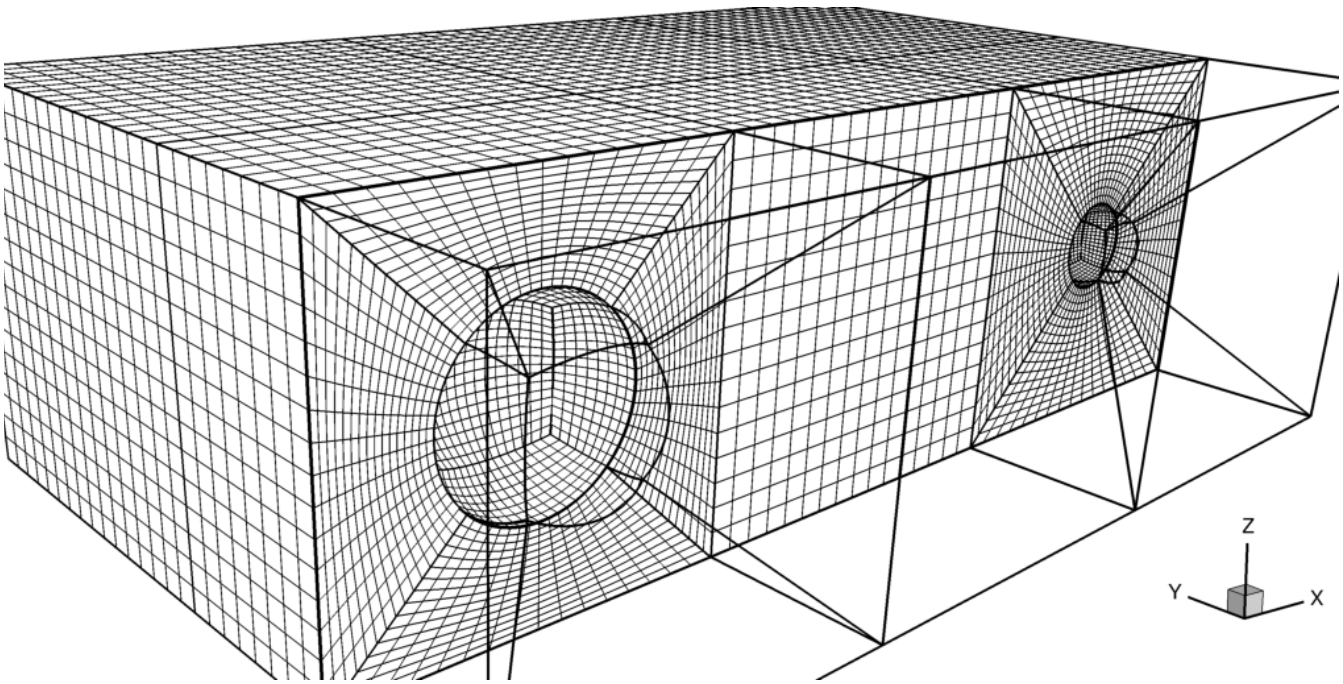


- we're also interested in potentially exploring weather/climate-type applications using our framework (perhaps fully 3D, non-hydrostatic)
- Earth mantle convection is another area of potential interest

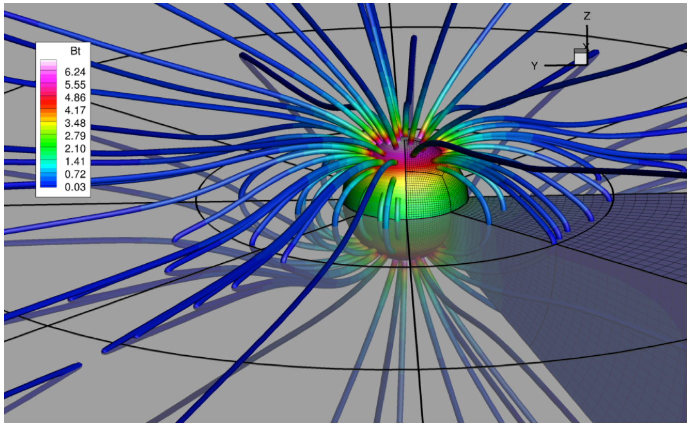


thank you

questions?